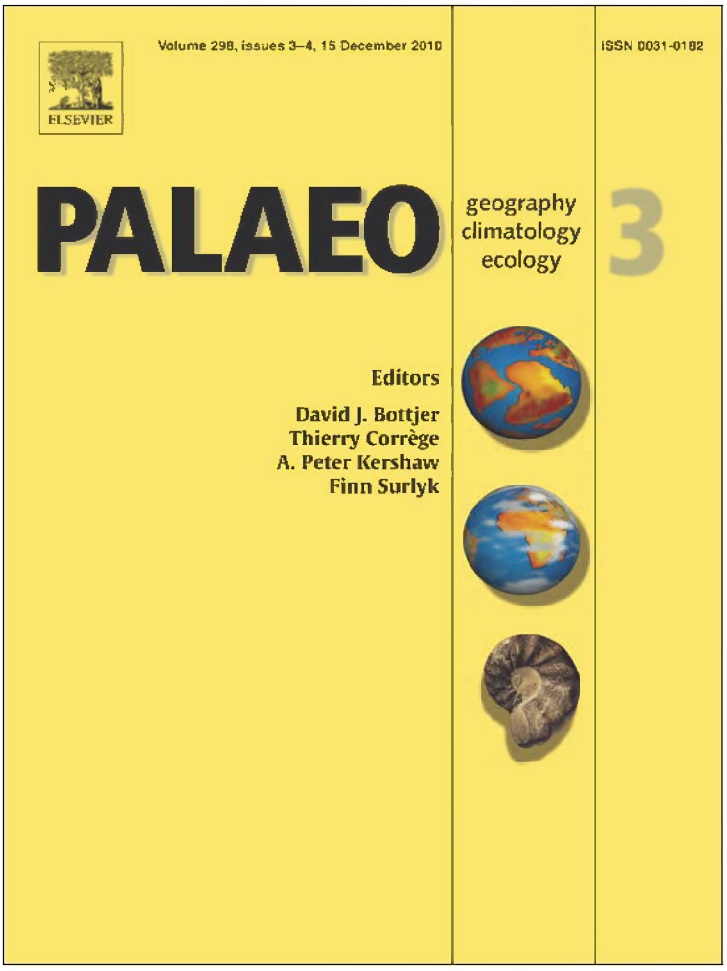

Palaeogeography, Palaeoclimatology, Palaeoecology 298 (2010) 319–340

Contents lists available at ScienceDirect

Palaeogeography, Palaeoclimatology, Palaeoecology

journal homepage: www.elsevier.com/locate/palaeo

Recent geographical distribution of organic-walled dinoflagellate cysts in the southeast Pacific (25–53°S) and their relation to the prevailing hydrographical conditions

Thomas J. Verleye *, Stephen Louwye

Research Unit Palaeontology, Department Geology and Soil Science, Ghent University, Krijgslaan 281 S8/WE13, 9000 Ghent, Belgium

ARTICLE INFO

Article history:
Received 9 February 2010
Received in revised form 22 September 2010
Accepted 10 October 2010
Available online 15 October 2010

Keywords:
Dinoflagellate cysts
Southeast Pacific
Quantitative reconstruction
Upwelling
Nutrient availability

ABSTRACT

Forty-eight surface sediment samples from the southeast (SE) Pacific (25–53°S) are investigated for the determination of the spatial distribution of organic-walled dinoflagellate cysts along the western South American continental margin. Fifty-five different taxa are recorded and reflect oceanic or coastal assemblages. The oceanic assemblages are characterised by low cyst concentrations and the dominance of autotrophs, while the coastal assemblages generally contain a higher number of cysts, which are mainly produced by heterotrophic species. Highest cyst concentrations are observed in the active upwelling system offshore Concepción (35–37°S). *Brigantedinium* spp., *Echinidinium aculeatum*, *Echinidinium granulatum/delicatum* and cysts of *Protoperidinium americanum* dominate assemblages related to upwelling. *Echinidinium aculeatum* appears to be the best indicator for the presence of all year round active upwelling cells. Other protoperidinioid cysts may also occur in high relative abundances in coastal regions outside active upwelling systems, if the availability of nutrients, co-responsible for the presence/absence of their main food sources such as diatoms and other protists, is sufficient. The importance of nutrient availability as a determining environmental variable influencing cyst signals on a regional scale (SE Pacific) is demonstrated through statistical analyses of the data. Because of the importance of nutrients, uncertainties about the outcomes of quantitative sea-surface temperature (SST) reconstructions (Modern Analogue Technique) based on dinoflagellate cysts may arise, since no interaction between different hydrographical variables is considered in this approach. The combination of the SE Pacific surface sample dataset with other published cyst data from the Southern Hemisphere resulted in a database which includes 350 samples: the 'SH350 database'. This database is used to test the accuracy of the quantitative reconstructions by calculating and comparing the estimated versus observed values for each site. An attempt to perform quantitative SST reconstructions on the last 25 cal ka of site ODP1233 (41°S; 74°27′W) is made and again stresses the importance of other environmental variables such as nutrient availability in determining the dinoflagellate cyst assemblages.

1. Introduction

Until now, the geographical distribution of dinoflagellate cysts and their controlling environmental factors in the SE Pacific Ocean are poorly understood. Except for the analysis of a few cores offshore Peru (Biebow, 2003; Wall et al., 1977) and a late Quaternary dinoflagellate cyst record offshore Mid-South Chile (Verleye and Louwye, 2010), no marine studies on dinoflagellate cysts are available. The sole study investigating the spatial distribution of cysts in the Chilean Fjord area between 43°S and 54°S is done by Alves-de-Souza et al. (2008). Dinoflagellate cyst studies during the last decennia mainly focused on the middle to high latitudes of the North Atlantic Ocean (e.g. Boessenkool et al., 2001a,b; de Vernal et al., 1994; de Vernal et al., 2001; Harland, 1983; Matthiessen, 1995; Rochon et al., 1999; Turon, 1984; Wall et al., 1977) since changes in the North Atlantic Deep Water production were generally accepted as the primary trigger for climate changes on orbital time scales (e.g. Broecker, 2003; Broecker and Denton, 1989; Clark et al., 2001; Imbrie et al., 1992, 1993; Seidov and Maslin, 2001; Vidal et al., 1999). Recently, new insights in millennial-scale climate change suggested also an active role for the Southern Hemisphere (SH) high latitudes in the initiation of rapid climate variability (Knorr and Lohmann, 2003; Stocker and Wright, 1991; Weaver et al., 2003). However, SH studies dealing with recent and late Quaternary dinoflagellate cysts are still rather rare (Alves-de-Souza et al., 2008; Benderra, 1996; Biebow, 2003; Esper and Zonneveld, 2002; Esper and Zonneveld, 2007; Harland and Pudsey, 1999; Harland et al., 1998; Marret and de Vernal, 1997; Marret et al., 2001; McMinn, 1992, 1995; McMinn and Sun, 1994; McMinn and Wells, 1997; Verleye and Louwye, 2010; Vink et al., 2000; Zonneveld et al., 2001).

* Corresponding author. Tel.: +32 9 264 46 09; fax: +32 9 264 46 08.
E-mail address: thomas.verleye@ugent.be (T.J. Verleye).

0031-0182/$ – see front matter © 2010 Elsevier B.V. All rights reserved.
doi:10.1016/j.palaeo.2010.10.006

The spatial distribution of dinoflagellate cysts in marine environments is considered to be mainly controlled by SST, sea-surface salinity (SSS) and the availability of nutrients (Dale, 1996; Dale et al., 2002; de Vernal et al., 1997; de Vernal et al., 2001; Devillers and de Vernal, 2000; Rochon et al., 1999). Several studies supported the use of the transfer function method applied to dinoflagellate cysts to quantify palaeo-SST, palaeo-SSS, sea ice cover and more recently nutrient availability (e.g. de Vernal et al., 1997, 2001, 2005; Marret et al., 2001; Rochon et al., 1999; Voronina et al., 2001). Guiot (1990) developed transfer functions based on the best analogue method (MAT; Modern Analogue Technique) for pollen data, later adapted by de Vernal et al. (1993, 1994) for dinoflagellate cyst assemblages of the Northern Hemisphere (NH). However, methodological aspects of the MAT, such as spatial autocorrelation within the training set, were questioned during the last decade (e.g. Dale, 2001; Jackson and Williams, 2004; Telford, 2006; Telford and Birks, 2005, 2009). The ecological basis of the transfer functions have been evaluated for dinoflagellate cysts as well as other microfossil groups such as diatoms and benthic foraminifers (e.g. Anderson, 2000; Murray, 2001). Dale (1983, 1996) demonstrated that cysts in coastal/neritic environments show consistent biogeographical distributions that might differ considerably from those observed in the adjacent deep-sea, notwithstanding a similar SST. Dale and Dale (1992) suggested that the observed differences might be related to large-scale lateral transport of cysts produced in coastal waters to the deep-sea. Furthermore, the species response model underlying the MAT assumes a linear relationship between an environmental gradient and the abundance of a particular species. A species however will often show an unimodal relationship to a specific environmental gradient as demonstrated by a.o. Whittaker (1973a,b).

This study provides the first extensive database of the geographical distribution of organic-walled dinoflagellate cysts from surface sediment samples in the SE Pacific. In order to compile a database which includes the spatial distribution of recent dinoflagellate cysts in the SH, the SE Pacific core-top samples were combined with surface sediment samples from earlier studies; this resulted in a database including 350 sites. This so called SH350 database was further used to gain insight into the underlying mechanisms and reliability of the MAT as a method for quantitative palaeoenvironmental reconstructions. This allows us to test if SSS and SST can be used as independent determining parameters, apart from other hydrographical variables and their mutual interactions, in order to make accurate quantitative palaeohydrographical reconstructions.

2. Regional settings

The eastward flowing Antarctic Circumpolar Current (ACC) dominates the surface water circulation of the SH high latitudes,

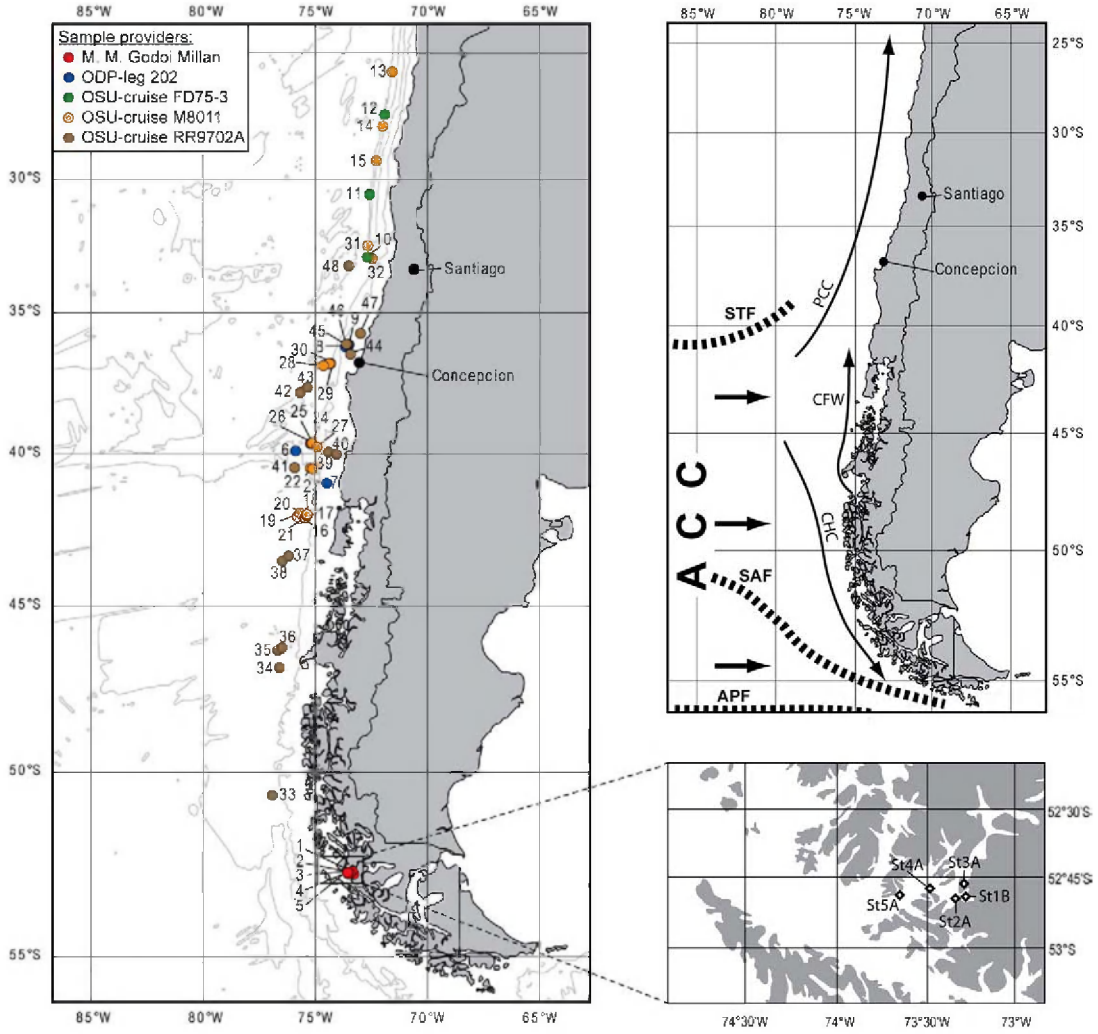

Fig. 1. Location of the 48 studied sites along the Chilean coast. Inset map of the fjord area in South Chile. The material derived from several institutions and cruises as indicated by the coloured dots. The upper right map visualises the main sea-surface oceanographic currents and circumpolar frontal systems. Abbreviations: ACC, Antarctic Circumpolar Current; CFW, Chilean Fjord Water; CHC, Cape Horn Current; PCC, Peru–Chile Current; APF, Antarctic Polar Front; SAF, Subantarctic Front; STF, Subtropical Front. Position of the circumpolar frontal systems after Belkin and Gordon (1996).

Table 1
Analysed surface samples inclusive the respective sea-surface hydrographical parameters.

Sample ID	Sample no.	Facility	Cruise	Sampling gear[a]	Lat.	Long.	Depth (m)	sSST (°C)[b]	wSST (°C)[b]	aSST (°C)[b]	sSSS (psu)[b]	wSSS (psu)[b]	aSSS (psu)[b]	sN[0m] (μmol/l)[c]	aN[0m] (μmol/l)[c]	aN[30m] (μmol/l)[c]	sP[0m] (μmol/l)[c]	aP[0m] (μmol/l)[c]	aP[30m] (μmol/l)[c]	sS[0m] (μmol/l)[c]	aS[0m] (μmol/l)[c]
1	St1B	M.A.G.M.	–	–	−52.78	−73.28	42	10.2	6.3	8.4	26.9	33.4	31.0	5.8*	5.8*	6.6*	0.92*	0.92*	0.80*	1.5	6.0
2	St2A	M.A.G.M.	–	–	−52.79	−73.29	60	10.2	6.3	8.4	26.9	33.4	31.0	5.8*	5.8*	6.6*	0.92*	0.92*	0.80*	1.5	6.0
3	St3A	M.A.G.M.	–	–	−52.75	−73.26	42	10.2	6.3	8.4	26.9	33.4	31.0	5.8*	5.8*	6.6*	0.92*	0.92*	0.80*	1.5	5.8
4	St4A	M.A.G.M.	–	–	−52.78	−73.48	22	10.3	6.3	8.4	27.0	33.4	31.0	5.8*	5.8*	6.6*	0.92*	0.92*	0.80*	1.5	5.9
5	St5A	M.A.G.M.	–	–	−52.79	−73.65	46	10.3	6.3	8.4	27.1	33.4	31.0	5.8*	5.8*	6.6*	0.92*	0.92*	0.80*	1.5	5.9
6	ODP 1232c	ODP	leg 202	pc	−39.88	−75.90	4075	16.7	11.7	14.0	33.8	33.7	33.4	3.5	4.0	6.4	0.40	0.66	0.74	2.8	2.7
7	ODP1233b	ODP	leg 202	pc	−41.00	−74.45	844	15.0	11.3	13.1	33.2	32.7	31.9	2.2	3.5	5.6	0.37	0.60	0.78	2.7	3.3
8	ODP1234a	ODP	leg 202	pc	−36.22	−73.68	1019	14.7	12.4	13.7	34.1	33.5	33.8	7.1	3.8	9.6	1.07	0.76	0.90	6.9	4.2
9	ODP1235a	ODP	leg 202	pc	−36.15	−73.57	494	14.5	12.4	13.7	34.1	33.5	33.8	7.1	3.8	9.6	1.07	0.76	0.90	7.0	4.3
10	FD75-3 01	OSU	FD75-3	gc	−32.96	−72.72	5584	17.0	13.4	15.0	34.3	34.1	34.2	8.5	5.1	6.4	0.77	0.70	0.81	2.7	2.5
11	FD75-3 03	OSU	FD75-3	gc	−30.57	−72.63	5862	17.7	13.7	15.5	34.4	34.3	34.3	6.2	4.0	5.8	0.39	0.48	0.60	1.7	1.9
12	FD75-3 04	OSU	FD75-3	gc	−27.47	−71.93	6154	19.4	14.4	16.6	34.7	34.6	34.6	2.7	2.2	6.1	0.42	0.44	0.66	1.0	1.9
13	M8011-1	OSU	M8011	pc	−25.70	−71.54	7725	20.8	15.5	17.7	34.8	34.7	34.7	0.2	2.2	6.4	0.75	0.53	0.68	1.1	1.9
14	M8011-2	OSU	M8011	gc	−27.91	−72.02	6451	18.9	14.3	16.3	34.6	34.5	34.5	7.0	2.9	8.5	0.31	0.48	0.62	1.1	1.9
15	M8011-3	OSU	M8011	gc	−29.28	−72.32	6442	17.8	13.7	15.5	34.5	34.4	34.4	7.7	3.8	6.9	0.22	0.43	0.56	1.6	2.2
16	M8011-4	OSU	M8011	pc	−42.11	−75.59	3847	15.1	10.7	12.9	33.2	33.4	33.0	2.9	3.8	6.1	0.35	0.56	0.69	1.8	2.6
17	M8011-5	OSU	M8011	gc	−42.07	−75.45	3854	14.9	10.6	12.8	33.2	33.3	32.9	2.9	3.8	6.1	0.35	0.56	0.69	1.8	2.7
18	M8011-7	OSU	M8011	pc	−42.07	−75.74	3819	15.2	10.7	12.9	33.3	33.4	33.0	3.1	3.9	6.2	0.36	0.58	0.70	1.8	2.7
19	M8011-8	OSU	M8011	pc	−42.04	−75.81	3810	15.4	10.8	12.9	33.4	33.4	33.1	3.2	4.0	6.2	0.35	0.59	0.70	1.9	2.7
20	M8011-9	OSU	M8011	pc	−41.97	−75.68	3819	15.3	10.8	13.0	33.4	33.4	33.0	3.1	3.9	6.2	0.36	0.58	0.70	2.0	2.8
21	M8011-10	OSU	M8011	gc	−42.08	−75.54	3850	15.0	10.6	12.9	33.2	33.3	33.0	2.9	3.8	6.1	0.35	0.56	0.69	1.8	2.7
22	M8011-11	OSU	M8011	gc	−40.48	−75.24	4101	15.8	11.4	13.5	33.5	33.3	32.8	3.0	3.7	6.0	0.45	0.64	0.77	2.6	2.9
23	M8011-12	OSU	M8011	pc	−40.50	−75.15	4137	15.7	11.4	13.5	33.5	33.1	32.8	2.9	3.7	5.9	0.45	0.64	0.79	2.6	2.9
24	M8011-13	OSU	M8011	pc	−39.66	−75.17	4413	16.3	11.7	13.9	33.7	33.4	33.1	3.2	3.8	6.6	0.57	0.70	0.71	3.0	2.8
25	M8011-14	OSU	M8011	gc	−39.66	−75.19	4307	16.3	11.7	13.9	33.7	33.4	33.1	3.2	3.8	6.6	0.57	0.70	0.71	3.0	2.8
26	M8011-15	OSU	M8011	gc	−39.67	−75.25	4219	16.3	11.7	13.9	33.7	33.4	33.1	3.2	3.8	6.6	0.57	0.70	0.71	3.0	2.8
27	M8011-16	OSU	M8011	gc	−39.75	−74.98	4338	16.1	11.7	13.8	33.7	33.3	32.9	3.1	3.9	6.6	0.53	0.71	0.82	3.0	2.8
28	M8011-17	OSU	M8011	gc	−36.90	−74.65	4787	16.0	12.6	14.3	34.0	33.6	33.8	4.2	2.8	9.3	0.87	0.78	0.86	4.9	3.1
29	M8011-18	OSU	M8011	pc	−36.85	−74.42	4608	15.6	12.5	14.1	34.0	33.6	33.7	4.2	2.8	9.3	0.87	0.78	0.86	5.1	3.3
30	M8011-19	OSU	M8011	gc	−36.87	−74.49	4727	15.8	12.6	14.1	34.0	33.6	33.7	4.2	2.8	9.3	0.87	0.78	0.86	5.1	3.3
31	M8011-20	OSU	M8011	gc	−32.52	−72.70	5994	17.3	13.5	15.1	34.3	34.2	34.2	7.7	4.8	5.3	0.68	0.66	0.73	2.1	2.3
32	M8011-21	OSU	M8011	pc	−33.01	−72.50	4024	16.9	13.4	14.7	34.3	34.2	34.2	9.1	5.4	6.8	0.80	0.72	0.85	2.8	2.6
33	RR9702A-01	OSU	RR9702A	mc	−50.65	−76.96	3964	10.7	7.5	9.1	32.3	32.2	32.2	8.7	10.6	10.3	1.06	1.08	1.09	0.1	2.5
34	RR9702A-06	OSU	RR9702A	mc	−46.88	−76.60	3298	12.8	9.0	10.8	32.8	32.6	32.2	8.0	7.7	9.3	0.48	0.93	0.91	1.4	3.2
35	RR9702A-08	OSU	RR9702A	mc	−46.35	−76.67	3014	13.0	9.0	11.0	32.6	32.7	32.1	6.9	6.6	6.4	0.43	0.84	0.84	1.5	3.2
36	RR9702A-10	OSU	RR9702A	mc	−46.32	−76.54	2879	13.0	9.1	11.0	32.4	32.5	32.1	6.5	6.3	8.2	0.41	0.83	0.84	1.5	3.3
37	RR9702A-12	OSU	RR9702A	mc	−43.42	−76.25	3523	14.7	10.1	12.4	33.0	33.4	32.8	3.5	4.4	6.3	0.40	0.59	0.69	1.4	2.7
38	RR9702A-14	OSU	RR9702A	mc	−43.54	−76.48	3471	14.7	10.1	14.3	33.1	33.3	32.8	3.9	4.7	6.5	0.42	0.62	0.71	1.5	2.7
39	RR9702A-20	OSU	RR9702A	mc	−39.97	−74.47	1055	15.3	11.4	13.4	33.5	32.8	32.2	2.8	3.8	6.2	0.49	0.89	0.84	2.9	3.0
40	RR9702A-22	OSU	RR9702A	mc	−40.01	−74.12	430	14.8	11.3	13.1	33.4	32.5	31.7	2.8	3.8	6.2	0.49	0.89	0.84	2.9	3.0
41	RR9702A-27	OSU	RR9702A	mc	−40.48	−75.92	3850	16.3	11.4	13.7	33.7	33.6	33.4	3.5	4.0	6.3	0.48	0.64	0.75	2.5	2.8
42	RR9702A-29	OSU	RR9702A	mc	−37.85	−75.75	4051	17.3	12.4	14.7	33.4	33.8	33.8	3.7	3.1	7.1	0.65	0.71	0.74	3.6	2.5
43	RR9702A-31	OSU	RR9702A	mc	−37.67	−75.43	3946	17.0	12.5	14.6	33.9	33.8	33.8	3.6	3.0	7.4	0.68	0.72	0.75	3.8	2.6
44	RR9702A-34	OSU	RR9702A	mc	−36.53	−73.45	133	13.7	12.1	13.1	34.1	33.4	33.7	7.7	4.1	9.9	1.22	0.81	0.88	7.3	4.5
45	RR9702A-39	OSU	RR9702A	mc	−36.17	−73.57	510	14.5	12.5	13.7	34.1	33.6	33.8	7.6	4.0	9.9	1.12	0.77	0.91	7.0	4.3
46	RR9702A-42	OSU	RR9702A	mc	−36.17	−73.68	1028	14.6	12.4	13.7	34.1	33.6	33.8	7.1	3.8	9.6	1.08	0.76	0.90	6.9	4.2
47	RR9702A-44	OSU	RR9702A	mc	−35.76	−73.01	172	13.9	12.2	13.4	34.1	33.5	33.8	7.6	3.9	9.9	1.03	0.75	0.93	6.4	4.0
48	RR9702A-46	OSU	RR9702A	mc	−33.28	−73.53	3852	17.4	13.8	15.7	34.3	34.1	34.2	6.5	4.0	5.4	0.63	0.63	0.72	3.2	2.6

[a]pc = piston core; gc = gravity core; mc = multicore.
[b]Data obtained from the World Ocean Atlas 2001 (quarter degree resolution) of the National Oceanographic Data Center (Stephens et al., 2002 [temperature]; Boyer et al., 2002 [salinity]). SST = sea surface temperature; SSS = sea surface salinity; a = annual; s = summer; w = winter.
[c]Data obtained from the World Ocean Atlas 2005 (one degree resolution) of the National Oceanographic Data Center (Garcia et al., 2006a [oxygen]; Garcia et al., 2006b [nutrients]). N = nitrate; P = phosphate.
*Estimated values, equated with nitrate and phosphate data from sample 13 of the Crucero Oceanografico CIMAR3 Fiordos (1998) (Palma and Silva, 2004; Valdenegro and Silva, 2003) at the entrance of the Strait of Magellan.

and is bounded to the north by the Subtropical Front. This frontal system separates the cold, nutrient-rich waters from the Subantarctic Zone in the south from the warm, nutrient-depleted waters from the Subtropical Zone in the north. Other circumpolar frontal systems located in the southern part of SE Pacific are the Subantarctic Front and the Antarctic Polar Front (Fig. 1).

The northward flowing Peru–Chile Current (PCC), also known as the Humboldt Current, dominates the surface water circulation off the west coast of South America (Fig. 1). This eastern boundary current originates between 40°S and 45°S, where the ACC approaches the South American continent and branches off in a northward (PCC) and a southward flowing current (Cape Horn Current; CHC) (Boltovskoy, 1976; Strub et al., 1998). Less than 100 km offshore, the less saline, northward flowing Chilean Fjord Water originates from the Patagonian fjords due to high annual rainfall associated with the onshore blowing westerlies (e.g. Villa-Martínez and Moreno, 2007).

The nutrient-rich but oxygen-poor southward flowing Gunther Under Current (GUC) underlies the PCC. This current transports Equatorial Subsurface Water at a water depth of 100 to 400 m (Fonseca, 1989) at an average speed 12.8 cm s^{-1} around 30°S (Shaffer et al., 1999), but diminishes in strength south of 33°S (Lamy et al., 2001). The oxygen-rich Antarctic Intermediate Water (AAIW) originates from subduction at the Antarctic Polar Front and flows northward (~1.1 cm s^{-1} at 30°S; Shaffer et al., 1999) at 400 to 1,200 m water depth. The Pacific Deep Water (PDW) is a slow, southward flowing current below 1,200 m water depth; it is in the deepest parts of the ocean underlain by the oxygen-rich Antarctic Bottom Water (AABW) (Garcia et al., 2006a; Ingle et al., 1980).

Perennial southerly winds result in Ekman-drift induced upwelling of cold, nutrient-rich water from the GUC between 32°S and 37°S, while upwelling between ~37°S and 40°S is restricted to the austral summer (Strub et al., 1998). The high supply of nutrients to the surface waters and related high biogenic primary production make that this region has an important impact on the global carbon cycle (Hebbeln et al., 2000).

3. Material and methods

3.1. Palynological lab treatments and analyses

3.1.1. SE Pacific samples

Forty-eight surface samples, originating from the western South American continental slope between 25°S and 53°S, were analysed. Sampling took place during cruises of the Joides Resolution (ODP leg 202), the Melville (Scripps Institution of Oceanography (SIO); cruises FD75-3 and M8011) and the Roger Revelle (SIO; cruise RR9702A). Five surface samples from the Chilean Fjord area nearby the Strait of Magellan were collected (March 2007) and provided by M. A. Godoi Millan (Cambridge University, UK).

Since only wet material was treated palynologically and used for the dinoflagellate cyst analysis, a surrogate sample helped to calculate the dry weight of the wet material. This precautious procedure was necessary, for the effect of drying techniques on the preservation of dinoflagellate cysts is still largely unknown. The wet weight of the surrogate samples ranges between 0.93 and 5.69 g, with an average of 2.33 g, resulting in dry weights between 0.42 and 3.59 g (average of 1.32 g). The wet sample weights range from 5.23 to 11.66 g with an average of 8.29 g. Using the dry:wet ratio from the respective surrogate sample, the dry weights of our samples were estimated from 1.45 to 9.38 g (average of 4.67 g). The *Lycopodium* marker-grain method was used to calculate the amount of cysts per gram of dry sediment (Mertens et al., 2009; Stockmarr, 1971). One to two *Lycopodium* tablets (batch no. 483216, x = 18,583) were added to each sample before the start of the acid treatments. The latter involved demineralisation with cold HCl (6%) for the removal of carbonates and cold HF (40%) for the dissolution of silicates (Louwye et al., 2004). The part of the organic fraction swept away during each decanting phase, was always recovered on a 10 μm mesh to prevent the loss of palynomorphs, in particular *Lycopodium* spores, for these tend to float (e.g. Salter et al., 2002). Mertens et al. (2009) demonstrated that ~24% of the *Lycopodium* spores were lost during decanting, which might cause considerable errors when calculating the cyst concentration per gram of dry sediment. The remaining organic fraction underwent a sonication treatment for 30 s. and was again sieved on a 10 μm mesh. The final residue was mounted on microscopy slides with glycerine jelly. A Zeiss Axioskop 2 Plus light microscope was used under 400 to 1,000x magnification for the identifications. At least 300 dinoflagellate cysts were counted in each sample, except in samples 11 (202 cysts) and 12 (262 cysts). In total 14,651 cysts were counted, with an average of 305 cysts/sample.

3.1.2. SH350 database

The SH350 database includes samples from eleven different core-top studies: Esper and Zonneveld (2002, 2007), Harland et al. (1998), Holzwarth et al. (2007), Marret (1994), Marret and de Vernal (1997), Marret et al. (2001), Vink et al. (2000), Zonneveld et al. (2001), Laurijssen and Zonneveld (unpublished) and this study. All studies used cold acid treatments including diluted HCl and HF. The mentioned studies used variable durations and numbers of treatment cycles but it is known that no selective degradation of dinoflagellate cysts occurs when using cold acids (Mertens et al., 2009). Differences in centrifugation time also have no influence on the preservation of cysts (Mertens et al., 2009).

Plate 1. Microphotographs of dinoflagellate cysts and other palynomorphs from the SE Pacific.

(1). Cyst type 11 (slide M8011-18, England Finder reference [EF] D43/0-1), optical section, high focus on expanded bases of processes, cyst diameter excluding processes 38 μm.
(2–3). Dinocyst sp. A (slide ODP1233-0 EF E45/2).
(2). High focus on granular surface and process bases which are composed out of several compartments.
(3). Optical section, focus on striate processes, orientation uncertain, cyst diameter exclusive of the processes 38 μm.
(4–5). Dinocyst sp. D (slide St2A EF B19/0).
(4). Optical section, surface covered by hair-like processes.
(5). High focus on archeopyle, cyst diameter excluding processes 37 μm.
(6). *Echinidinium* sp. 4 (slide RR9702A-06 EF D24/0), orientation uncertain, cyst diameter exclusive of the spines 25 μm.
(7–9). *Impagidinium* sp. 1 (slide FD75-3-04(2) EF U18/3).
(7). Optical section, focus on membranes.
(8). High focus on sulcal area, ventral view.
(9). Combined low foci , dorsal view, archeopyle, maximum cyst diameter exclusive of the membranes 41 μm.
(10). *Selenopemphix* sp. 1 (slide RR9702A-10 EF B44/4), optical section with antapical view, archeopyle in low focus, cingulum characterised by undulated margins, maximum cyst diameter 57 μm.
(11). *Spiniferites* sp. 5 (slide FD75-3-04(2) EF P16/2), optical section, processes always broken, tabulation similar to *Spiniferites* species, orientation uncertain, maximum cyst diameter exclusive of processes 45 μm.
(12). *Impagidinium cantabrigiense* (slide M8011-13(2) EF G28/0), optical section. Scale bars 20 μm.

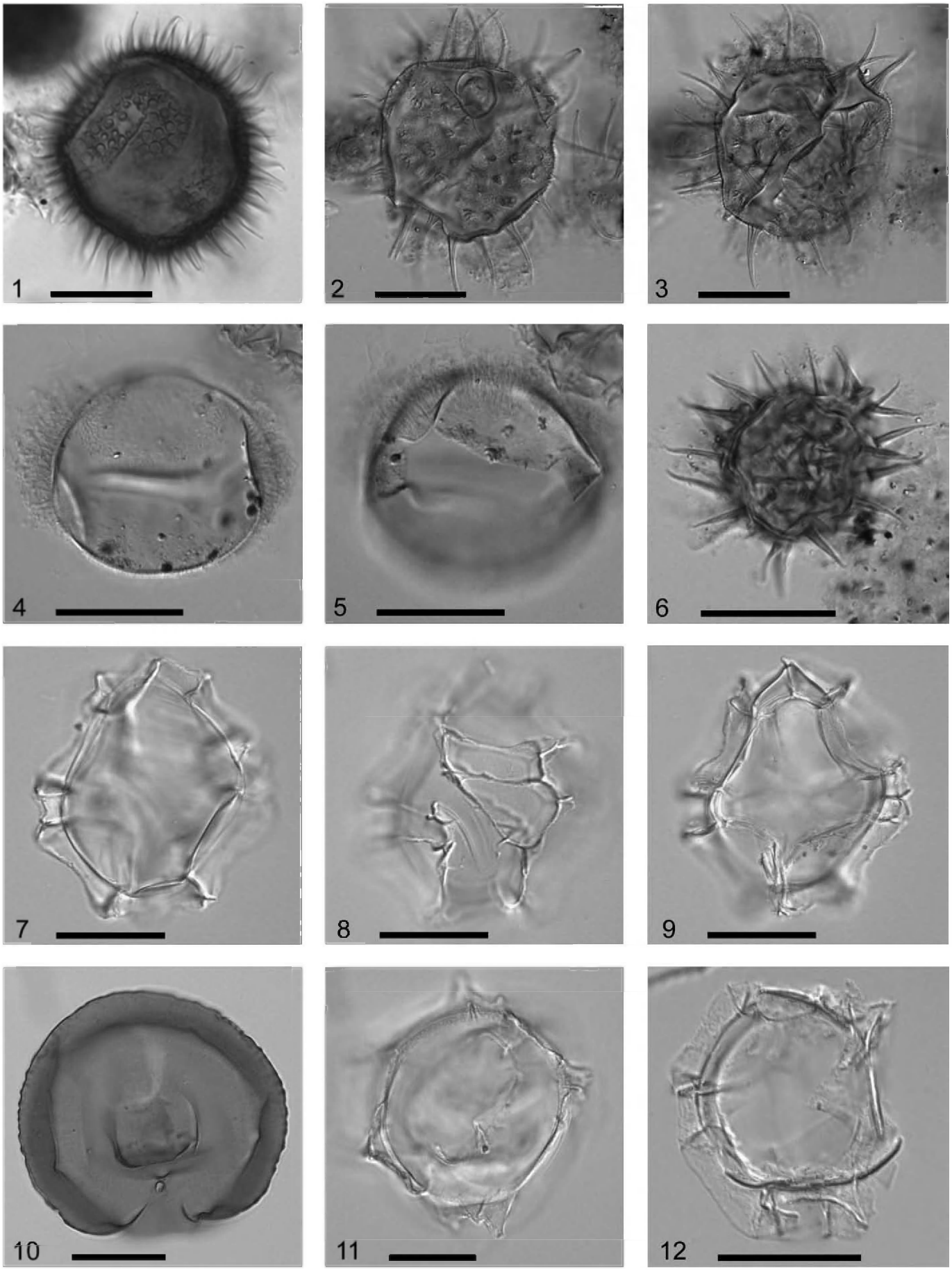

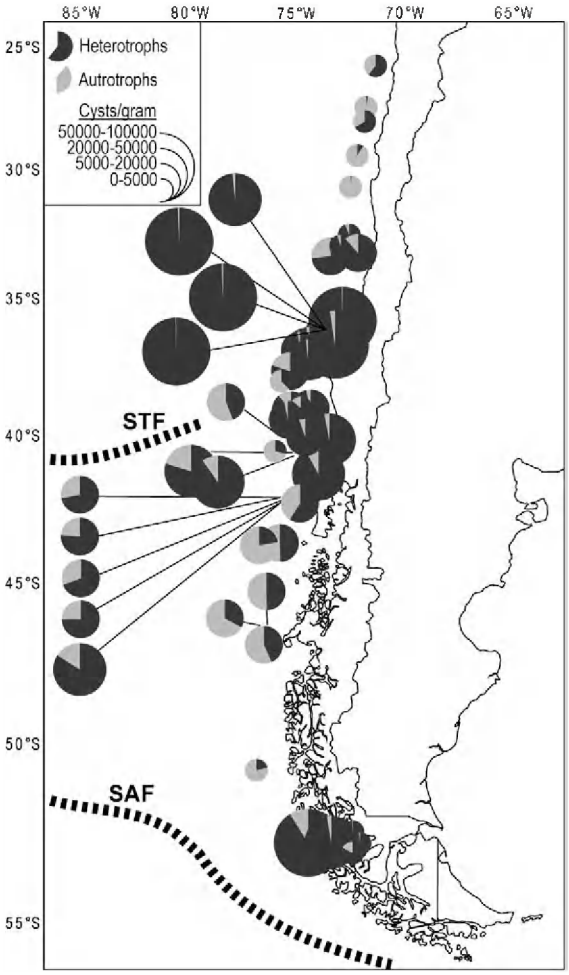

Fig. 2. Dinoflagellate cyst concentrations along the Chilean continental margin, inclusive the relative amount of heterotrophic versus autotrophic taxa.

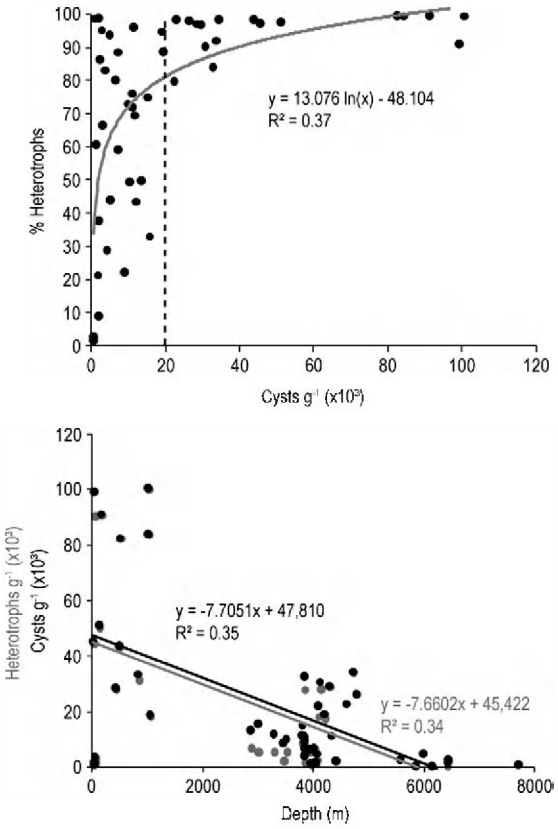

Fig. 3. The relative amount of cysts produced by heterotrophic taxa plotted against dinoflagellate cyst concentrations; the cyst concentrations and absolute abundances of heterotrophs in relation with water depth.

However, different sieving techniques were used in the SH surface sample studies. Both nylon meshes of 10 μm and Storck-Veco (mesh 508) precision sieves with round pores of exactly 20 μm diameter were used. Mertens et al. (2009) and Lignum et al. (2008) demonstrated that sieves with mesh widths up to 15 μm result in an insignificant loss of cysts. The aperture size of a mesh is measured along the *x* and *y*-axes and the diagonal aperture of a 15 μm mesh measures 21.3 μm, but taking into account the irregularity of a nylon mesh, it might be slightly smaller or larger (Lignum et al., 2008). Therefore, meshes with a diagonal aperture up to 21.3 μm result in a negligible loss of dinoflagellate cysts, and the difference in cyst loss between a 10 μm nylon mesh (diagonal aperture of 14.2 μm) and a Storck Veco precision sieve of 20 μm is negligible, as already mentioned by Holzwarth et al. (2007).

Since the somewhat different palynological treatments and sieving techniques do not result in differences in preservation and cyst loss, the samples can be combined to form a SH dinoflagelle cyst core-top database and the SH350 database can be used to test the accuracy of the MAT.

3.2. Taxonomy

The taxonomy follows Rochon et al. (1999) and Fensome and Williams (2004). However, the cyst orientations and their preservation were not always favourable and a number of specimens have been identified only to genus level, grouped as *Achomosphaera* spp., *Brigantedinium* spp., *Impagidinium* spp., *Lejeunecysta* spp., *Polykrikos* spp. or *Spiniferites* spp. *Brigantedinium* spp. represent the following three taxa: *Brigantedinium cariacoense*, *Brigantedinium simplex* and Cyst form C (Wall et al., 1977). Specimens not identifiable to genus level were grouped as 'indeterminate gonyaulocoids' or 'protoperidinioids'. *Echinidinium granulatum* and *Echinidinium delicatum* were grouped as *Echinidinium granulatum/delicatum*. The nomenclature predating Matsuoka et al. (2009) was used for the determination of the *Polykrikos* taxa.

The dinoflagellate cyst assemblages from the SE Pacific are still poorly documented. A few new morphotypes belonging to the genera *Echinidinium*, *Impagidinium*, *Selenopemphix* and *Spiniferites*, were identified (Appendix A). An abundant cyst, Cyst type 11, is not considered to be a dinoflagellate cyst since no morphological features, such as a visible archeopyle, or culture experiments, are available to classify this cyst within the division Dinoflagellata.

3.3. Environmental parameters

The one-degree resolution data of the World Ocean Atlas 2005 of the National Oceanographic Data Center (Garcia et al., 2006a [oxygen]; Garcia et al., 2006b [nutrients]) provided the present day nitrate, phosphate, silica and oxygen concentrations (Table 1). The annual and seasonal salinity and temperature data were obtained from the quarter-degree resolution data of the World Ocean Atlas 2001 (Stephens et al., 2002 [temperature]; Boyer et al., 2002 [salinity]) (Table 1). The average annual SSTs in the study area vary between 8 and 18 °C. Austral winter (July to September) minima are observed in the vicinity of the Strait of Magellan (52.8°S) with SSTs of

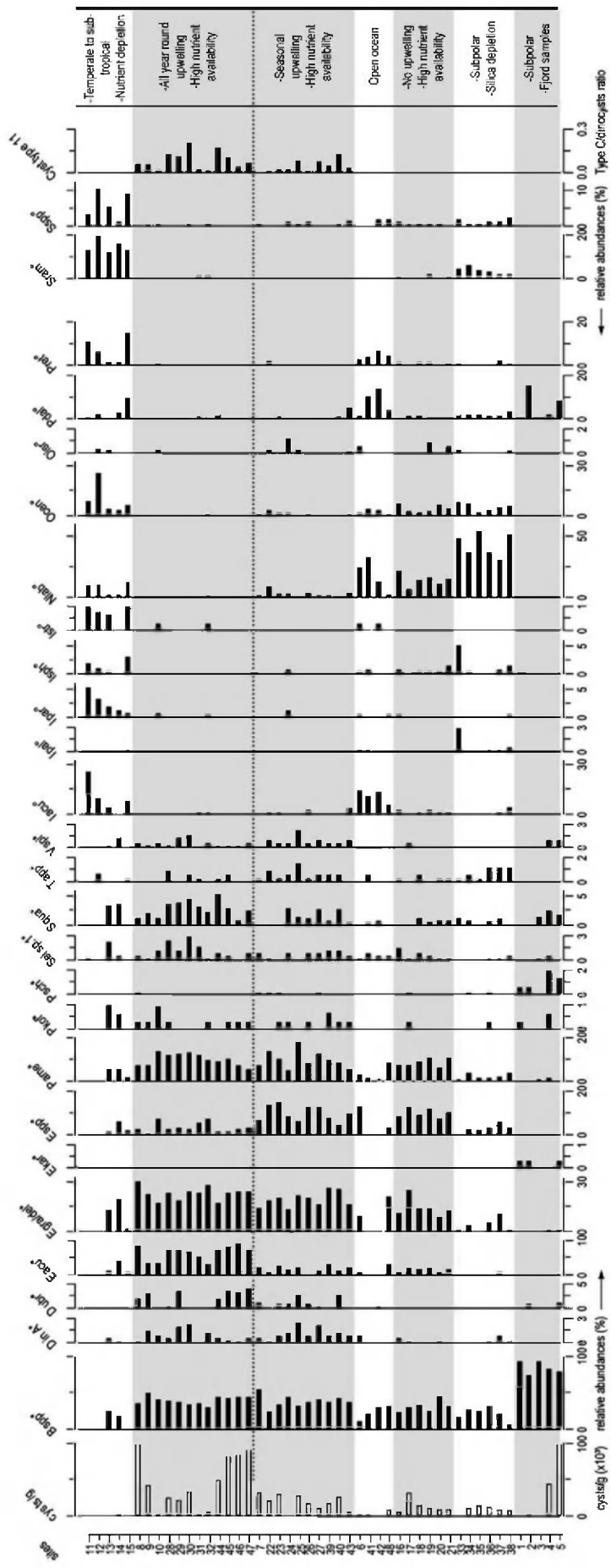

Fig. 4. Relative abundances of the main dinoflagellate cyst taxa at the different sampling sites. Dinoflagellate cyst/g are also given. The abundances of Cyst type 11 are shown as the 'Cyst type 11/dinocysts' ratio. Sites are grouped according to their geographical position. (*) heterotrophs; (°) autotrophs. Abbreviations: Bspp, *Brigantedinium* spp.; Din A, Dinocyst sp. A; Dukr, *Dubridinium caperatum*; Eacu, *Echinidinium aculeatum*; Egra/del, *Echinidinium granulatum/delicatum*; Ekar, *Echinidinium karaense*; Espp, *Echinidinium* spp. indet.; Iacu, *Impagidinium aculeatum*; Ipal, *Impagidinium pallidum*; Ipar, *Impagidinium paradoxum*; Ispa, *Impagidinium sphaericum*; Istr, *Impagidinium striatum*; Nlab, *Nematosphaeropsis labyrinthus*; Ocen, *Operculodinium centrocarpum*; Oist, *Operculodinium israelianum*; Pame, cysts of *Protoperidinium americanum*; Pdal, cysts of *Pentapharsodinium dalei*; Pkof, cysts of *Polykrikos kofoidii*; Psch, cysts of *Polykrikos schwartzii*; Pret, *Pyxidinopsis reticulata*; Sel sp. 1, *Selenopemphix* sp. 1; Squa, *Selenopemphix quanta*; Sram, *Spiniferites ramosus*; Sspp, *Spiniferites* spp. indet.; Tapp, *Trinovantedinium applanatum*; Vspi, *Votadinium spinosum*.

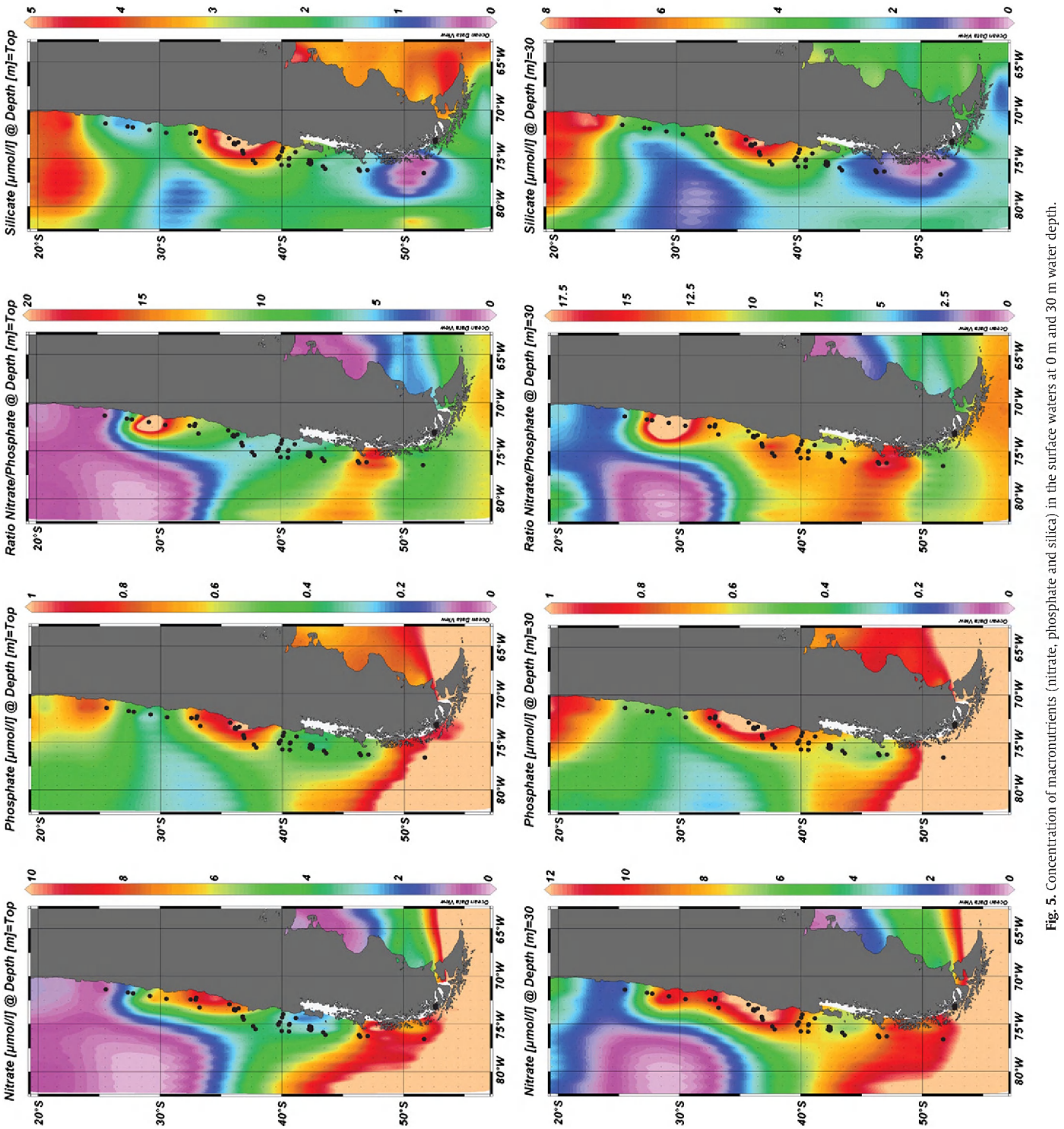

Fig. 5. Concentration of macronutrients (nitrate, phosphate and silica) in the surface waters at 0 m and 30 m water depth.

~6 °C, while maxima of ~16 °C are found at the location of the northernmost sample (25.7°S). Austral summer (January to March) SSTs vary between 10 and 21 °C. The SST reflects a clear N–S gradient, but intense upwelling of cold water along the western South American coast (32–37°S) during austral summer also causes a steep east–west SST gradient of 3 to 4 °C with only a 2° shift in longitude.

SSS shows a much narrower range. The oceanic samples, except samples 1 to 5, all have an average annual SSS range between 31.7 and 34.7 psu. According to the World Ocean Atlas 2001, samples 1 to 5 (Chilean fjord) have an austral summer SSS of 26.9 psu and an austral winter SSS of 33.4 psu. However, salinity in fjords show a rapid increase with depth from fresh/brackish water at the top (upper meter <15 psu) to high saline water (~30 psu) at 10 m water depth (M. A. Godoi Millan, unpublished).

3.4. Statistical analyses

The statistical approach of the dataset was performed using the R-software 2.7.0 (R Development Core Team, 2008) and the CANOCO 4.02 for Windows software (ter Braak and Šmilauer, 1998). Ordination techniques were used to reduce the multidimensionality of the dataset by taking into account the covariance structure of the data. A Detrended Correspondence Analysis (DCA; Hill, 1979) was performed in order to determine the underlying response model of the species distribution to the changing environmental parameters (see Supplementary data 1). Non-transformed relative abundances of the dinoflagellate cyst taxa were used as the input for the ordinations. The first DCA axis has a length of 2.86 standard deviations, which supports the assumption of an unimodal species response model (>2 SD; ter Braak, 1995), rather than a linear model. An unimodal curve for ordination allows the estimation of an 'optimum' and the ecological 'tolerance' of the species. A multivariate direct gradient analysis, Constrained Correspondence Analysis (CCA; Jongman et al., 1987; Ter Braak, 1986, 1987), was performed. This means that the available environmental variables are explicitly incorporated in the analysis. The conditional effect, which is the amount of variability explained by only one particular variable (eliminating covariance), is calculated through forward selection. The significance of each environmental parameter was determined through Monte Carlo testing, based on 499 unrestricted permutations. The species distribution on the CCA ordination plot was compared with the distribution pattern on the unconstrained CA (see Supplementary data 2). This enables us to make an independent assessment of the extent of contribution of the environmental variables included in the CCA to the cyst signals. On the ordination diagram, environmental parameters are shown by arrows pointing in the direction of maximum variation, while their length demonstrates the relative importance of the particular parameter. The centre of the plot indicates the mean value for each environmental parameter. The degree of correlation between environmental variables is visualised by the angle between the environmental arrows: the greater the angle, the less likely they are related to one other. The perpendicular projection of the species or sample points onto an environmental arrow gives the position of the abundance optimum of that species or sample on the variable (ter Braak and Prentice, 1988).

3.5. Modern Analogue Technique—database extension and accuracy

The SH350 database was used in order to quantify the accuracy of the MAT as a technique for quantitative palaeoenvironmental reconstructions of sea-surface conditions. About three transformations of the relative abundances per taxa were performed in order to compare the differences in precision of the MAT validation exercises: (1) no transformation, and the (2) log [% + 1] and (3) log [(%x 10) + 1] logarithmic transformations. The latter data transformation is in agreement with the procedure introduced by de Vernal et al. (2001). It includes a representation of the relative abundance data in per thousand to avoid decimals which would result in negative logarithmic values. Thereby, 'one' is added to the frequency of each taxon to avoid null values for taxa with no occurrence in the dataset. Logarithmically transformed relative abundances give more weight to species with lower occurrences, which are often associated with a narrower range of environmental conditions and thus good indicator species. All three datasets are separately used to calculate the distances or degree of similarity between each sample from the SH350 database, and the selection of the best analogues. This enables us to select the best data transformation method for palaeoenvironmental reconstructions. In this study, five analogues were considered to estimate the hydrographical conditions of a particular site. An environmental variable is estimated by calculating the average of this variable from the analogue sites, weighted inversely to the distance of the analogues. Plotting the estimated versus observed hydrographical data in a scatter plot gives an indication of the accuracy of the reconstruction according to de Vernal et al. (1997). The more the linear equation approximates $y = x$ (lowest Root Mean Square Error [RMSE]) with $R^2 = 1$, the better the environmental reconstruction should be.

4. Results

4.1. Spatial distribution of taxa

Forty-eight surface samples were analysed for organic-walled dinoflagellate cysts in order to determine their spatial distribution in the SE Pacific (Fig. 1). A total of 55 taxa were distinguished (Appendix A). Twenty-eight species are heterotophic, 26 autotrophic and one has an unknown affinity (Dinocyst sp. D; Plate 1 Figs. 4–5). The most prominent heterotrophs are *Brigantedinium* spp. (0–90%), several *Echinidinium* species (0–42%) and cysts of *Protoperidinium americanum* (0–18%). Dinocyst sp. A (Plate 1 Figs. 2–3), *Lejeunecysta* spp. indet., *Polykrikos kofoidii*, *Polykrikos schwartzii*, *Quinquecuspis concreta*, *Selenopemphix quanta*, *Selenopemphix* sp. 1 (Plate 1 Fig. 10), *Trinovantedinium applanatum* and *Votadinium spinosum* are much less frequent (<5%). The main constituents of the autotrophic assemblages are *Impagidinium* species (0–45%), *Nematosphaeropsis labyrinthus* (0–56%), *Operculodinium centrocarpum* (0–26%), cysts of *Pentapharsodinium dalei* (0–16%), *Pyxidinopsis reticulata* (0–15%) and *Spiniferites* species (0–31%) (see Supplementary data 3).

The cyst concentration per gram of sediment varies between 525 ± 52 and 100,753 ± 17,205, while the relative amount of heterotrophic taxa fluctuates between 1.5 and 99.7% (Figs. 2 and 3). Both the total cyst concentrations and the absolute abundances of heterotrophic species display a prominent decrease with increasing water depth (i.e., increasing distance from the shore) (Fig. 3). Areas characterised by high cyst concentrations (>20,000) in their sediments are always dominated by heterotrophs (>80%), regions with lower cyst concentrations (<20,000) show a varying ratio of heterotrophic and autotrophic taxa (Fig. 3).

Low cyst concentrations characterise the five most equatorward sites (11–15) (Fig. 1). Three of them have an assemblage which is almost completely autotrophic, dominated by *Impagidinium aculeatum*, *Nematosphaeropsis labyrinthus*, *Operculodinium centrocarpum* and *Spiniferites ramosus* (Figs. 2 and 4). The sites between 33 and 42°S are dominated by the heterotrophic *Brigantedinium* spp., *Echinidinium aculeatum*, *Echinidinium granulatum/delicatum* and cysts of *Protoperidinium americanum* (Fig. 4). Very high cyst concentrations of more than 50,000 cysts per gram are found offshore Concepción (35–37°S) (Fig. 2), an area characterised by year-round upwelling resulting in high nitrate, phosphate and silica concentrations in the surface waters (Fig. 5). South of the Subtropical Front, *Nematosphaeropsis labyrinthus* becomes more dominant (up to 50%), but its frequency is still restricted in the near-coastal samples between 40 and 42°S (Fig. 4). The most poleward

sites in the Chilean Fjord area near the entrance of the Strait of Magellan are dominated by *Brigantedinium* spp. (>80%) (Fig. 4). The only autotrophs recorded in this area were cysts of *Pentapharsodinium dalei* and a single specimen of *Operculodinium centrocarpum* (Fig. 4).

Notable is the occurrence of a single specimen of *Impagidinium cantabrigiense*. This species was recorded and described by De Schepper and Head (2008) from the Pliocene/Pleistocene section of DSDP Hole 610A (53°13.30′N; 18°53.21′W). The oldest finds of the species date from the latest Pliocene (1.86 Ma), its youngest occurrence from the Middle Pleistocene (0.53 Ma). However, the sample corresponding with the age of 0.53 Ma is the highest sample processed from Hole 610A, and younger occurrences of the species are not excluded. The single *Impagidinium cantabrigiense* specimen at site 24 suggests that the species may not be extinct, although it may also be a rare reworked specimen.

4.2. Constrained Correspondence Analysis

The overall inertia (variance) in the species dispersion is 1.145 while the amount of the total variation explained by the environmental variables, the sum of constrained eigenvalues (explainable inertia), is 0.816 (Fig. 6a and b, Table 2). The first two CCA-axes combined explain 45.6% of the variance in the species distribution, while they explain 64% of the total explainable inertia (Table 2). The species distributions on the CA and CCA ordination plots are very similar (Supplementary data 2); this suggests that the environmental factors expressed in the CCA have a major influence on the dinoflagellate cyst distribution (Dale and Dale, 2002). The environmental variables significantly correlated ($P<0.05$) with the CCA axes, are the annual mean and summer mean silica concentrations in the surface waters (aS[0 m]; sS[0 m]), the mean sea-surface temperature during austral winter (wSST), the summer and annual mean sea-surface salinity (sSSS; aSSS) and the annual mean nitrate concentrations at the surface (aN[0 m]) and at 30 m water depth (aN[30 m]) (Table 3). The strength of each variable is expressed by the Lambda A values, of which the sum corresponds with the explainable inertia (Table 3).

Six distributional site groupings were identified from the ordination diagram (A–F; Fig. 6b) which correspond to the environmental groups visualised in Fig. 4: (A) the most equatorward sites characterised by low nutrient concentrations; (B) upwelling region with high nutrient supply; (C) no upwelling, nutrients available but in lower concentrations compared with the upwelling and fjord areas; (D) most poleward oceanic samples, high availability of nitrate and phosphate but low silica concentrations; (E) open oceanic sites, restricted nutrient availability; (F) fjord samples, high nutrient concentrations.

The first CCA axis (CCA1) shows a contrast between the heterotrophic cysts which plot at the negative side of CCA1 and the autotrophic cysts plotting positively (Fig. 6a). The nutrient rich fjord and upwelling sites are ordinated at the negative side of CCA1 (Groups B and F), while sites characterised by a depletion of one or more macronutrients are plotted positively (Groups A, D and E) (Fig. 6b). At the negative side, CCA1 is best correlated with silica and phosphate concentrations in the surface waters, at the positive side with water depth (Fig. 6a and b, Table 4). However, when considering the seperate effect of the environmental factors by eliminating the covariance between environmental parameters (=conditional effects), phosphate concentrations and water depth seem to be less important variables (Table 3). The reason for this is the negative correlation between water depth and nutrient concentrations (mainly silica), and the latter are known to have a considerable impact on the dinoflagellate cyst assemblages (Table 4). Therefore, the observed changes in cyst assemblages with variable water depth (or distance from the shore) are most likely the result of a change in nutrient availability rather than water depth itself.

Fig. 7 shows that CCA1 explains almost entirely the variation in the relative amount of heterotrophs in the assemblages ($R^2=0.98$), with lowest CCA1 scores for high productive, nutrient rich upwelling areas. The amount of variance in the species distribution explained by CCA1 is largest for the following species: *Brigantedinium* spp. (49%), *Nematosphaeropsis labyrinthus* (49%), *Operculodinium centrocarpum* (44%), *Spiniferites ramosus* (35%), *Dubridinium caperatum* (32%), *Spiniferites* spp. indet (28%), *Impagidinium aculeatum* (26%), *Echinidinium aculeatum* (25%), *Impagidinium paradoxum* (21%), *Echinidinium granulatum/delicatum* (20%) and *Selenopemphix quanta* (20%) (Table 5).

The second axis is strongly correlated with SSS and SST (Fig. 6a and b, Table 4). The highest positive scoring end-members on CCA2 are temperate to tropical species such as *Impagidinium aculeatum*, *Impagidinium paradoxum*, *Impagidinium strialatum*, *Spiniferites mirabilis* and *Spiniferites ramosus*, which have highest relative abundances in Group A (Fig. 6a, b). Cold water species such as *Echinidinium karaense*, *Impagidinium pallidum*, *Nematosphaeropsis labyrinthus* and *Polykrikos schwartzii* plot most negatively and show highest relative abundances in Groups D and F (Fig. 6a and b). Considering the conditional effects of the variables, only the average winter SST and the annual and summer mean SSS correlate significantly with the CCA axes (Table 3). The taxa showing the best fit with CCA2, representing SST, are *Impagidinium strialatum* (40%), *Nematosphaeropsis labyrinthus* (34%), *Impagidinium paradoxum* (31%), *Pyxidinopsis reticulata* (26%), *Spiniferites ramosus* (21%) and *Spiniferites* spp. (21%) (Table 5).

The percentage fit by all environmental variables combined shows that the given environmental parameters explain >60% of the distribution of *Brigantedinium* spp. (88%), *Nematosphaeropsis labyrinthus* (86%), *Echinidinium aculeatum* (85%), *Spiniferites ramosus* (84%), *Impagidinium pallidum* (81%), *Echinidinium granulatum/delicatum* (72%), *Impagidinium plicatum* (72%), *Selenopemphix quanta* (71%), *Dubridinium caperatum* (68%), *Impagidinium strialatum* (68%), cysts of *Protoperidinium americanum* (64%) and Dinocyst A (63%) (Table 5).

4.3. Modern Analogue Technique

A validation exercise was performed to test the accuracy of the MAT as a technique for quantitative reconstructions of palaeohydrographical changes. The SH350 database was used as a training set to estimate SSS and SST of all sites, in order to compare these results with the observed values (Fig. 8a, b, c, d and e). The smaller the RMSE (the mean difference between the observed and estimated values), the better the reconstruction should be. The non-transformed dataset of the relative abundances gives the lowest RMSEs for both SSS and SST (winter–summer) (Fig. 8b, c, d, and e, Table 6). The least good fits result from the log([%x10]+1) dataset transformation (Table 6). This

Fig. 6. Plots showing the results of the first two axes of the Constrained Correspondence Analysis (CCA) ordination diagram, species and sites separately visualised. a) Only the taxa with a total occurrence in the dataset of more than three specimens are considered. Abbreviations of environmental variables: a, annual; w, winter; s, summer; P, phosphate; N, nitrate; S, silica; SSS, sea-surface salinity; SST, sea-surface temperature. Abbreviations of species names: ACHO, *Achomosphaera* spp.; BSPP, *Brigantedinium* spp.; BTEP, *Bitectatodinium tepikiense*; DINA, Dinocyst sp. A; DUBR, *Dubridinium caperatum*; EACU, *Echinidinium aculeatum*; EGRA, *Echinidinium granulatum/delicatum*; EKAR, *Echinidinium karaense*; ESPP, *Echinidinium* spp. indet.; IACU, *Impagidinium aculeatum*; IPAL, *Impagidinium pallidum*; IPAR, *Impagidinium paradoxum*; IPAT, *Impagidinium patulum*; IPLI, *Impagidinium plicatum*; ISPH, *Impagidinium sphaericum*; ISPP, *Impagidinium* spp. indet.; ISTR, *Impagidinium strialatum*; LSPP, *Lejeunecysta* spp.; NLAB, *Nematosphaeropsis labyrinthus*; OCEN, *Operculodinium centrocarpum*; OISR, *Operculodinium israelianum*; PAME, cysts of *Protoperidinium americanum*; PDAL, cysts of *Pentapharsodinium dalei*; PERI, Indeterminate protoperidinioids; PKOF, cysts of *Polykrikos kofoidii*; PSCH, cysts of *Polykrikos schwartzii*; PRET, *Pyxidinopsis reticulata*; QCON, *Quinquecuspis concreta*; SELSP1, *Selenopemphix* sp. 1; SQUA, *Selenopemphix quanta*; SMIR, *Spiniferites mirabilis*; SRAM, *Spiniferites ramosus*; SSPP, *Spiniferites* spp. indet.; TAPP, *Trinovantedinium applanatum*; VSPI, *Votadinium spinosum*. b) Site numbers. The site distribution on the CCA plot results in the identification of 6 groups (A–F), corresponding to their geographical distribution.

indicates that weighting of rare species with narrow ecological ranges does not result in better estimations, but rather the opposite.

When dividing the SE Pacific sites in multiple clusters in a similar way as Telford (2006) did (Fig. 9), most of the analogues of the non-transformed database are selected within the same cluster (75% at average; max. 92%; min. 32%), and average 63% (max. 80%; min. 24%) within a range of 2.5° longitude/latitude (Table 7). Almost the same results are obtained with the log(%+1)-transformed database. When the

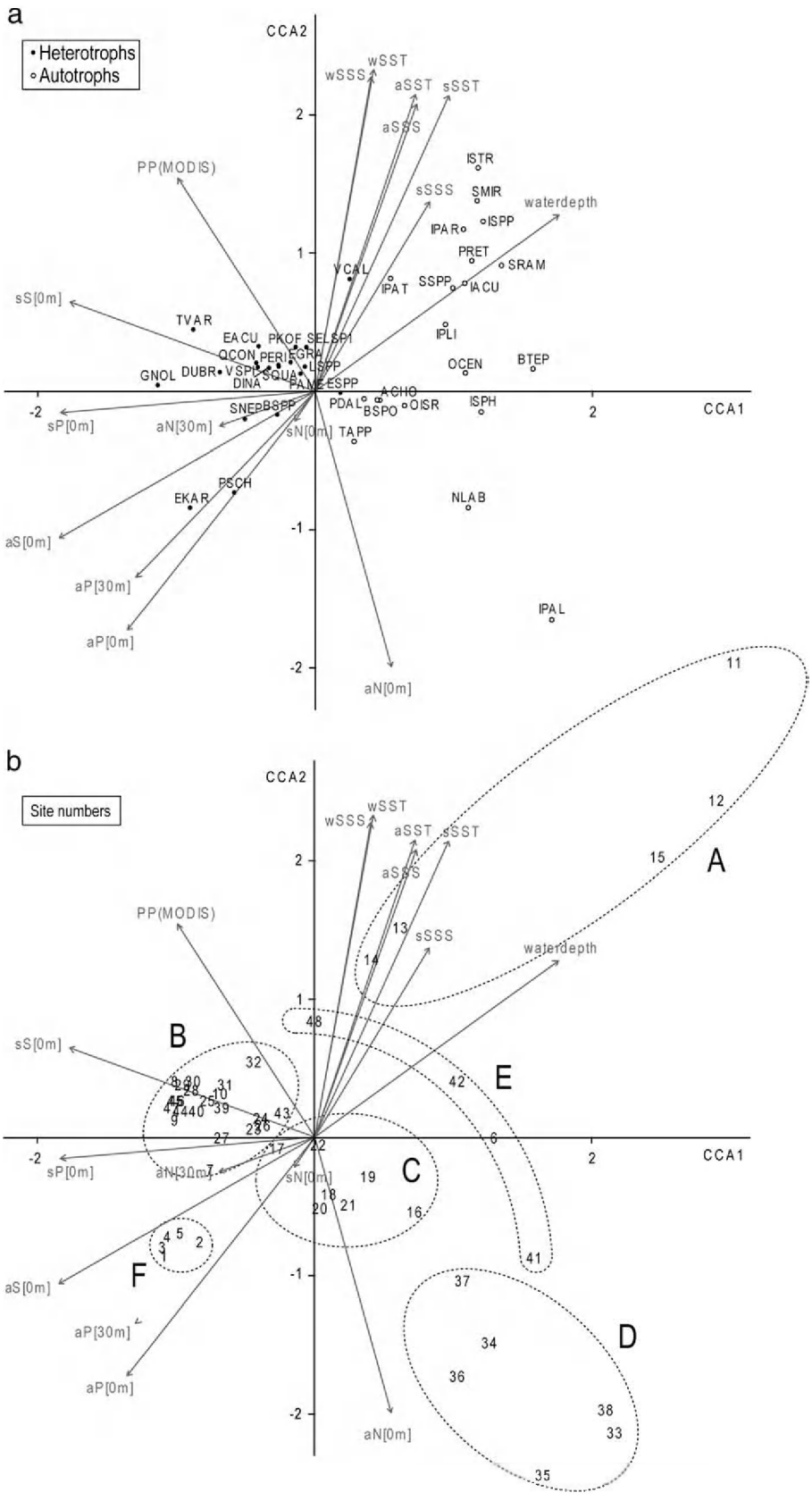

Table 2
Eigenvalues for the first four CCA axes; species-environment correlation; cumulative percentage variance of species data; cumulative percentage variance of species-environment relation; sum of all eigenvalues; sum of all constrained eigenvalues.

CCA	CCA axes				
	Axis 1	Axis 2	Axis 3	Axis 4	Total intertia
Eigenvalues	0.341	0.181	0.13	0.069	1.145
Species-environment correlations	0.877	0.946	0.91	0.926	
Cumulative percentage variance					
of species data	29.8	45.6	56.9	62.9	
of species-environment relation	41.8	64	79.9	88.4	
Sum of all eigenvalues					1.145
Sum of all canonical eigenvalues					0.816

Table 3
Significance of the given environmental variables in determining the nature of species distribution.

Environmental parameters	Significance		
	Lambda1	LambdaA	P-value
Marginal effects[a]			
aSilica[0 m]	0.21		
waterdep	0.17		
sSilica[0 m]	0.17		
sSST	0.16		
aSST	0.16		
wSST	0.16		
sPO4[0 m]	0.15		
sSSS	0.15		
aPO4[0 m]	0.15		
aSSS	0.14		
PP (MODIS)	0.14		
wSSS	0.13		
aPO4[30 m	0.12		
aNO3[0 m]	0.11		
aNO3[30 m]	0.06		
sNO3[0 m]	0.02		
Conditional effects[b]			
aSilica[0 m]		0.21	*0.002*
wSST		0.16	*0.002*
sSilica[0 m]		0.11	*0.002*
aNO3[30 m]		0.06	*0.002*
aSSS		0.04	*0.022*
sSSS		0.05	*0.010*
sPO4[0 m]		0.02	0.072
waterdep		0.03	0.072
PP (MODIS)		0.02	0.072
aNO3[0 m]		0.03	*0.032*
aSST		0.02	0.092
sNO3[0 m]		0.02	0.110
sSST		0.02	0.078
aPO4[30 m]		0.01	0.414
wSSS		0.01	0.622
aPO4[0 m]		0.01	0.708

[a] Marginal effects represent the amount of variance explained by the variable, uncorrected for covariance.
[b] Conditional effects represent the amount of variance explained by a particular variable only (i.e. the unique effect of the variable on the species composition). The P-values are indicative for the significance of the variable (at the 5% significance level, $P \leq 0.05$).

data are transformed as suggested by de Vernal et al. (2001), the number of analogues selected in the immediate vicinity decrease to an average of 63% within the same cluster and 55% within a 2.5° range (Table 7).

5. Discussion

5.1. Geographic distribution of organic-walled dinoflagellate cysts related to environmental conditions

5.1.1. Transport and preservation

A debated issue in the domain of dinoflagellate cyst palaeoecology concerns the effects of transport and of preservation on the accuracy of palaeoenvironmental reconstructions (e.g. Dale, 1976; Dale, 2001; Dale and Dale, 1992; Mudie, 1992; Zonneveld and Brummer, 2000; Zonneveld et al., 1997; Zonneveld et al., 2001). Transport and preservation may cause misinterpretation when associating dinoflagellate cyst assemblages in core-top samples with the prevailing environmental conditions in the above lying surface waters. To test whether horizontal transport of dinoflagellate cysts occurred offshore Chile, the cyst associations of adjoining sites at different water depths were compared. If lateral transport had occurred, the cysts from the deepest samples would be formed further away from the respective sites compared with the shallower ones because of the longer sinking period. So one would expect different assemblages originating from different locations at the adjoining sampling sites. Sites 8, 9 and 44 to 47 are located at depths between ~100 and ~1,100 m around 36.5°S (Fig. 1, Table 1). All cyst assemblages are very similar and show high cyst concentrations dominated by *Brigantedinium* spp. and *Echinidinium* species (Fig. 4). These data indicate that only negligible lateral transport occurred in the surface and subsurface waters (PCC, GUC, and AAIW) of the SE Pacific. This is in agreement with data from Shaffer et al. (1999, 2004), demonstrating that the AAIW moves too slowly to cause resuspension of sediments. The similar assemblages at sites 10, 31 and 32 (~33°S; Fig. 1) situated at water depths between 4,000 and 6,000 m also excludes transport by bottom water currents (PDW and AABW) which is in agreement with the observations of Ingle et al. (1980). Further evidence for negligible lateral transport in the studied area is the good match between the cyst assemblages and the hydrographical boundaries as visualised in Fig. 4. Additionally, almost no reworked palynomorphs were recorded, which may indicate negligible sediment transport.

The overall preservation of the palynomorphs was good but selective degradation cannot be excluded with absolute certainty in all samples. The five northernmost samples (11–15) (Fig. 1) are located in the deep parts of the Peru–Chile trench at depths of ~6,000 m and more (Table 1). The low cyst concentrations and high relative amount of resistant autotrophic cysts between 25°S and 31°S may be caused by selective degradation, related to higher bottom oxygen concentrations associated with the AABW (Garcia et al., 2006a; Ingle et al., 1980). The low concentrations of either nitrate, phosphate or silica in the surface waters between 25°S and 31°S during austral summer could also be controlling factors for the low cyst production (Fig. 5). A depletion of phosphate prevents diatoms to proliferate, even when nitrate and silica are present in quantity (Egge, 1998). Diatoms become also scarce when silica is depleted (Abrantes et al., 2007; Kilham, 1971). Since diatoms form an important source of nutrition for heterotrophic dinoflagellates (e.g. Jacobson and Anderson, 1986), protoperidinioid cysts are observed only in low concentrations. Mechanical degradation of cysts as the result of turbidity currents must also be considered and turbidity flows are known to occur preferentially along submarine slopes at active convergent plate margins such as the Peru–Chile trench (Blumberg et al., 2008). The poorly preserved cysts of *Operculodinium centrocarpum*, a species moderately sensitive for oxygenic degradation (Zonneveld et al., 1997), let us assume that degradation processes occurred after deposition at sites 15 and 41. The oxygen-rich AABW could be the reason for the poor preservation of the sensitive protoperidinioid cysts in the southernmost oceanic sample (33) (Fig. 1); this may lead to an overestimation of the relative amount of autotrophs. Higher relative abundances of heterotrophic cysts were expected south of 43°S based on the increasing nitrate and phosphate concentrations. However, lower concentrations were observed with respect to the sites north of 43°S. The reason for this is most likely the silica depleted surface waters occurring south of 43°S, rather than a preservational issue (Fig. 5). The geographical fit between the silica depleted surface waters

Table 4
Correlation matrix of environmental parameters and the CCA axes.

Environmental parameters	Sp ax1	Sp ax2	Env ax1	Env ax2	aSST	aSSS	wSST	wSSS	sSST	sSSS	depth	sN [0 m]	sP [0 m]	aN [0 m]	aN [30 m]	aP [0 m]	aP [30 m]	sS [0 m]	aS [0 m]
Sp ax2	0.07	1.00																	
Env ax1	0.88	0.00	1.00																
Env ax2	0.00	0.95	0.00	1.00															
aSST	0.22	0.70	0.25	0.74	1.00														
aSSS	0.22	0.68	0.25	0.71	0.91	1.00													
wSST	0.12	0.74	0.14	0.78	0.98	0.93	1.00												
wSSS	0.13	0.76	0.14	0.80	0.64	0.72	0.63	1.00											
sSST	0.29	0.70	0.33	0.74	0.97	0.85	0.93	0.66	1.00										
sSSS	0.25	0.45	0.28	0.47	0.88	0.84	0.89	0.29	0.82	1.00									
depth	0.53	0.42	0.60	0.44	0.67	0.64	0.60	0.52	0.78	0.58	1.00								
sN [0 m]	−0.05	−0.07	−0.05	−0.07	−0.21	0.09	−0.09	0.05	−0.32	−0.10	−0.23	1.00							
sP [0 m]	−0.55	−0.05	−0.63	−0.05	−0.27	−0.03	−0.14	0.01	−0.41	−0.26	−0.52	0.50	1.00						
aN [0 m]	0.17	−0.65	0.19	−0.69	−0.72	−0.56	−0.69	−0.54	−0.70	−0.49	−0.29	0.56	0.20	1.00					
aN [30 m]	−0.21	−0.08	−0.24	−0.09	−0.07	0.19	0.05	−0.15	−0.23	0.14	−0.26	0.51	0.66	0.15	1.00				
aP [0 m]	−0.41	−0.56	−0.47	−0.59	−0.73	−0.63	−0.65	−0.61	−0.77	−0.57	−0.65	0.38	0.63	0.65	0.43	1.00			
aP [30 m]	−0.39	−0.44	−0.44	−0.46	−0.42	−0.26	−0.29	−0.54	−0.54	−0.14	−0.54	0.46	0.72	0.50	0.70	0.81	1.00		
sS [0 m]	−0.53	0.21	−0.61	0.22	0.24	0.37	0.36	0.06	0.06	0.34	−0.37	0.24	0.62	−0.38	0.64	0.15	0.46	1.00	
aS [0 m]	−0.56	−0.35	−0.64	−0.37	−0.76	−0.65	−0.69	−0.27	−0.82	−0.81	−0.84	0.30	0.64	0.32	0.26	0.66	0.44	0.24	1.00
PP	−0.30	0.50	−0.34	0.53	0.57	0.60	0.68	0.30	0.40	0.60	−0.03	0.33	0.30	−0.40	0.38	−0.17	0.21	0.68	−0.16

and the lower concentration of *Protoperidinium* cysts supports negligible lateral transport of cysts in the studied region. At the entrance of the Strait of Magellan (~53°S), similar nitrate and phosphate but higher silica concentrations (~9 μmol/l) with respect to the southernmost oceanic sites were measured by Valdenegro and Silva (2003). Here, extremely high cyst concentrations, between 50,000 and 100,000 cysts per gram, were observed (samples 4 and 5), dominated by *Brigantedinium* spp. (80–90%). This may point to the positive influence of silica availability in the surface waters for the spatial distribution of protoperidinioid cysts.

5.1.2. Spatial distribution of dinoflagellate cyst taxa

The geographical distribution of the taxa (Fig. 4) and their position in the CCA ordination plot allows to distinguish oceanic and coastal/neritic assemblages (Fig. 6). Warm, cold and upwelling related assemblages are also distinguished. Based on the CCA plot, the oceanic assemblages are dominated by autotrophic dinoflagellate cysts and low cyst concentrations, while coastal/neritic environments are dominated by heterotrophic taxa and high cyst concentrations (Fig. 3). This confirms the results of a.o. Boessenkool et al. (2001b), Bouimetarhan et al. (2009), Dale et al. (2002), Holzwarth et al. (2007), Pospelova et al. (2008). The available surface samples allowed us to study two coast–ocean transects over ~2° longitude (74°W–76°W) at 40°S and 41°S, respectively, to point out the possible effect of water depth and the covarying nutrient concentrations on the cyst composition (Fig. 10). The SSS of the most coastward sample in both transects is ~1.5 psu lower compared with that of the oceanic sites, while temperature slightly decreases in the immediate vicinity of the coast (ΔSST = 0.9 [1] and 0.6 [2]). Nevertheless, we observed an obvious shift from heterotrophic dominated assemblages to autotrophic dominated assemblages with increasing distance from the coast (Fig. 10). In both transects, the most prominent change in the cyst association occurs between 75°W and 76°W, the coast being located at 74°W. This excludes SSS and SST as triggers for the changing cyst compositions along both transects, but points at the importance of nutrient availability which decreases with increasing distance from the shore. This is in agreement with the observations of a.o. Dale et al. (2002).

Both the oceanic and coastal assemblages contain species associated with cold environments, such as *Echinidinium karaense*, *Impagidinium pallidum*, *Nematosphaeropsis labyrinthus*, *Polykrikos schwartzii* and *Selenopemphix antarctica* (Fig. 4). As to the warm water species, it is difficult to determine whether the presence of these species is conditioned by warmer surface waters or nutrient depletion, because the five most equatorward sites, characterised by the highest SST, have very low macronutrient concentrations in the surface waters. In the case of *Pyxidinopsis reticulata*, the high relative abundances of this species at the most northward sites may be related with macronutrient depletion rather than with increasing SST (Fig. 4); at sites south of Australia (50°S; Marret and de Vernal, 1997) characterised by mean annual SSTs of <10 °C, this species is well represented. Species which seem to be more related with warmer surface waters are *Impagidinium paradoxum*, *Impagidinium strialatum*, *Spiniferites mirabilis* and *Spiniferites ramosus* (Fig. 4).

The active coastal upwelling zones (Fig. 5) are characterised by the dominance of *Brigantedinium* spp., *Echinidinium aculeatum*, *Echinidinium granulatum/delicatum* and cysts of *Protoperidinium americanum*. Other taxa occurring in highest abundances in the immediate vicinity of active upwelling cells are Dinocyst sp. A, *Dubridinium caperatum*, *Echinidinium* sp. 4, *Selenopemphix quanta*, *Selenopemphix* sp. 1 and *Votadinium spinosum*. The observed dominance of protoperidinioid taxa in coastal upwelling systems and the presence of fewer autotrophic species which are largely out-competed by diatoms (Dale, 1996; Dale et al., 2002) accords with the results of previous studies (Dale, 1996; Dale et al., 2002; Holzwarth et al., 2007; Marret, 1994; Marret and Zonneveld, 2003; Pitcher and Joyce, 2009; Pospelova et al., 2008; Sprangers et al., 2004; Susek et al., 2005; Wall et al., 1977; Zonneveld, 1997; Zonneveld et al., 2001). However,

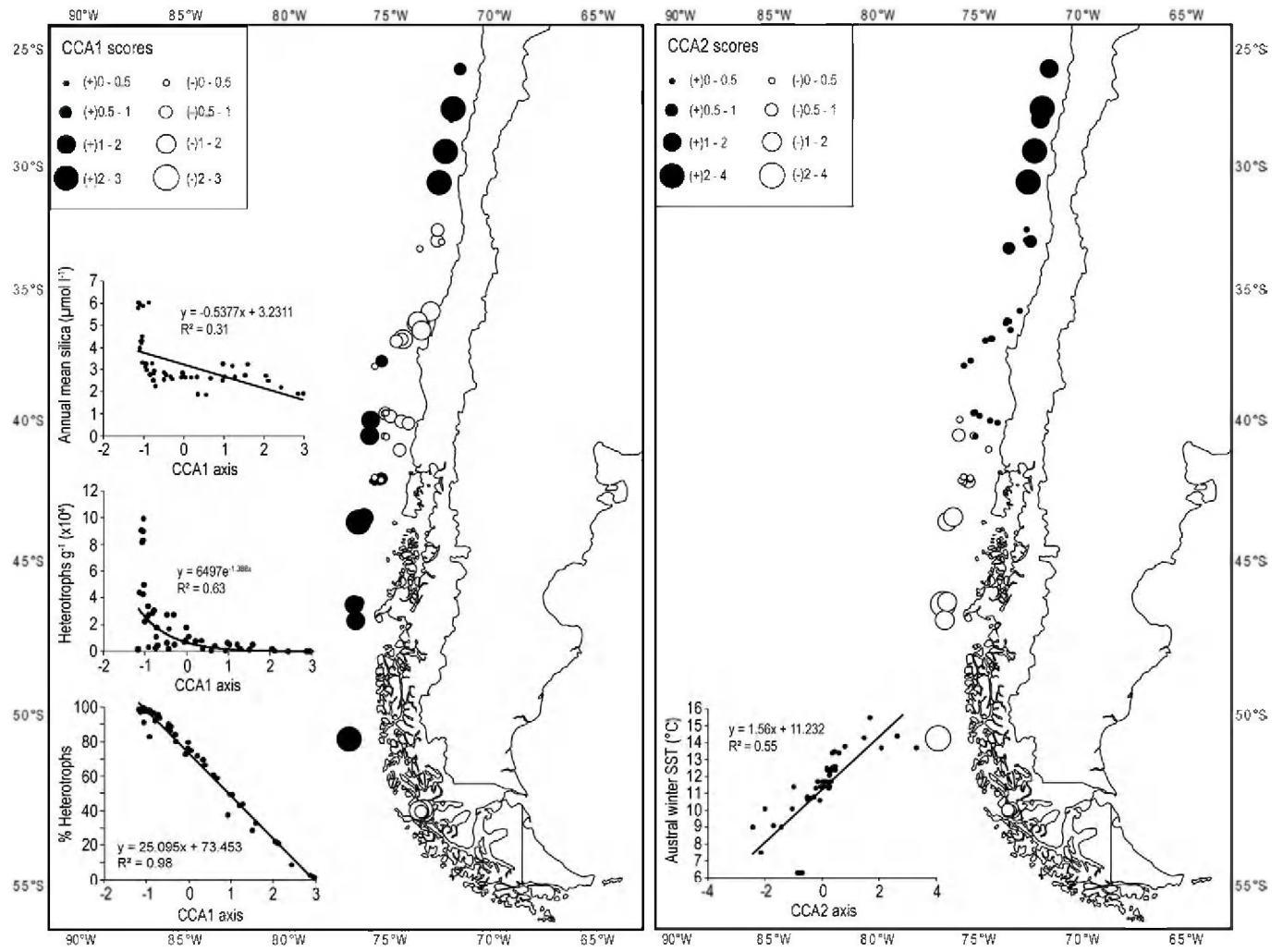

Fig. 7. Geographical plot of the scores of the first two CCA axes. The relationship between CCA1 and silica availability, heterotrophic taxa per gram and relative abundances of heterotrophs is visualised. A scatter plot showing the relationship between CCA2 and the austral winter SST is also shown.

not all these taxa are necessarily linked to active coastal upwelling cells, such as *Brigantedinium* spp., which is fairly a cosmopolitan genus. *Echinidinium granulatum/delicatum* and cysts of *Protoperidinium americanum* show highest concentrations in active upwelling systems, but also occur in relatively high numbers in regions without upwelling along the Chilean coast, on condition that dissolved macronutrients are sufficiently available in the upper water column (Fig. 4). According to the present study, the best markers for the detection of active upwelling of nutrient rich water are *Echinidinium aculeatum* and Cyst type 11 (Fig. 4, Plate 1 Fig. 1). Although *Echinidinium aculeatum* does not occur in very high relative abundances (6–10%) in upwelling regions, an obvious increase is observed between 32°S and 37°S with respect to other coastal regions (Fig. 4).

The CCA output confirms the importance of dissolved nutrients in the euphotic zone as the main triggering environmental variables for protoperidinioid taxa (Figs. 6 and 7). The variance in the relative abundances of heterotrophic taxa is almost perfectly explained by the first CCA axis ($R^2 = 0.98$) (Fig. 7), mainly representing water depth and nutrient availability (Fig. 6, Table 4). Remarkably, the increasing concentration of dissolved nitrate in the surface waters in active upwelling regions does not result in a correlation of its vector with the heterotrophic taxa in the CCA ordination plot. The reason lies in the increasing concentrations of surface water nitrate south of 43°S. A depletion of silica south of 43°S most likely leads to lower concentrations of protoperidinioids and results in a deviation of the mean annual surface water nitrate concentration vector in the CCA plot to colder sites and their associated species (Fig. 6).

5.2. Constraints on the applicability of dinoflagellate cyst based quantitative palaeohydrographical reconstructions

The MAT applied to dinoflagellate cysts is a transfer function method used in palaeoceanography for the quantification of palaeohydrographical changes during the Quaternary. The main presupposition of the MAT is that similar dinoflagellate cyst assemblages derive from similar environments and that the environmental variables used are ecologically important (Birks, 1995). So far, the method has been used mainly to reconstruct SSS and SST (e.g. de Vernal and Hillaire-Marcel, 2000; de Vernal and Pedersen, 1997, 2001, 2005; Marret et al., 2001), as SSS and SST are generally considered to be the main ecological parameters determining overall species distributions. In this case, cyst assemblages are regarded as a function of SSS or SST only, excluding any form of interaction between these and other environmental parameters. This approach differs fundamentally from the statistical methods used in ecological studies. The biogeographical distribution of species is related to the intricate interaction of biological and environmental factors, making it often difficult to assess the extent to which a particular variable influences the spatial distribution of a taxon (Dale and Dale, 2002).

To test the suitability of the MAT for palaeoenvironmental reconstructions in the SH, particularly in the SE Pacific, a validation

Table 5
Cumulative fit per dinoflagellate cyst species as fraction of variance of species. The values indicate to which extent a particular axis explains the variation in the distribution of a particular species (perfect fit = 1). The last column shows the percentage fit of all environmental variables together.
Underlined values: more than 20% of total species variance explained by respective axis.

Taxa	CCA axes				
	Axis 1	Axis 2	Axis 3	Axis 4	% Expl
Achomosphaera spp.	0.00	0.00	0.01	0.01	24
Brigantedinium spp.	0.49	0.56	0.87	0.88	88
B. tepikiense	0.13	0.13	0.14	0.17	42
Dinocyst A	0.14	0.17	0.40	0.41	63
D. caperatum	0.32	0.33	0.40	0.40	68
E. aculeatum	0.25	0.36	0.59	0.61	85
E. granulatum/delicatum	0.20	0.31	0.69	0.69	72
E. karaense	0.07	0.11	0.52	0.54	58
I. aculeatum	0.26	0.44	0.49	0.68	69
I. pallidum	0.16	0.33	0.34	0.35	81
I. paradoxum	0.21	0.52	0.53	0.54	58
I. patulum	0.04	0.18	0.19	0.19	55
I. plicatum	0.41	0.42	0.42	0.42	72
I. sphaericum	0.16	0.36	0.41	0.50	59
I. strialatum	0.18	0.58	0.61	0.62	68
Lejeunecysta spp.	0.02	0.04	0.14	0.14	36
N. labyrinthus	0.49	0.83	0.86	0.86	86
O. centrocarpum	0.44	0.45	0.45	0.50	59
O. israelianum	0.07	0.07	0.08	0.09	28
Cysts of *P. americanum*	0.11	0.16	0.54	0.56	64
Cysts of *P. dalei*	0.02	0.02	0.27	0.28	41
P. kofoidii	0.04	0.09	0.09	0.24	41
P. reticulata	0.29	0.55	0.59	0.62	67
P. schwartzii	0.09	0.18	0.51	0.54	61
Q. concreta	0.12	0.14	0.23	0.23	53
S. quanta	0.20	0.25	0.32	0.46	71
Selenopemphix sp. 1	0.06	0.18	0.28	0.28	59
S. mirabilis	0.07	0.18	0.18	0.20	35
S. ramosus	0.35	0.55	0.56	0.83	84
Spiniferites spp. indet.	0.28	0.48	0.49	0.57	61
T. applanatum	0.02	0.11	0.27	0.27	46
V. spinosum	0.19	0.22	0.26	0.28	53

exercise compared the observed and estimated SST and SSS (summer and winter), considering only the closest five analogues (Fig. 8b, c, d, and e). According to de Vernal et al. (1997), the correlation between estimated and observed SSS and SST leads to a quantification of the accuracy of the MAT. The striking correlation between the observations and estimations give the impression that the MAT is capable to perform SSS and SST reconstruction with high accuracy. However, the background data show a geographical clustering of the analogues in the immediate vicinity of the sites from which the SSS and SST are estimated, as also observed by Telford (2006). Therefore, five clusters which enclose restricted geographical areas were distinguished in the SE Pacific (Fig. 9) in a similar way as done by Telford (2006). Using the non-transformed relative abundance dataset, i.e., best fit between estimations and observations (Table 6), 75% of the analogues were selected within the same cluster, while 63% were found within a range of 2.5° longitude/latitude (Table 7). Taking these results into account, the good fit between observed and estimated values is rather unsurprising. Within a 2.5° range, and even within the clusters, environmental variables such as SSS, SST, nutrient availability and light regime remain fairly unchanged in a oceanic environment. Therefore, as also demonstrated by Telford (2006), any variable varying less within clusters than between clusters will appear possible to reconstruct, irrespective of its ecological relevance. In that case, the reconstruction of nitrate and phosphate contents, and to a lesser extend even water depth, also result in good fits between observed and estimated values (Fig. 8f, g, and h). Also, the MAT does not consider the interaction of the ecological parameters. As already shown, the high availability of dissolved macronutrients in the active upwelling area off Concepción results in high cyst concentrations and almost entirely heterotrophic assemblages. However, south of 43°S, the high nitrate and phosphate concentrations do not result in high cyst concentrations and protoperidinioid-dominated assemblages, most likely because of the silica depleted surface waters preventing diatoms to bloom (Kilham, 1971). This example points to the importance of considering interactions of parameters. Although SSS and SST are probably the most important environmental parameters influencing the distribution of dinoflagellate cysts on a global scale, on a regional scale, other variables such as availability of nutrients, water depth, light regimes, water stability etc. may be equally or even more important. Therefore, salinity and temperature should not be considered independent of the other ecological variables. In order to illustrate the importance of other parameters and their mutual interactions in the reconstructions, the cyst assemblages of several modern sites with a comparable SSS and SST, located randomly over the SH, were compared (Fig. 11). In the three comparisons, totally different assemblages were detected at sites with similar SSS and SST. An increase in the availability of macronutrients seems to increase the amount of heterotrophs in the assemblages (Fig. 11). The silica depleted surface waters west off Tasmania (Garcia et al., 2006b) probably caused the low protoperidinioid concentrations at site TAS67GC46 (Marret and de Vernal, 1997), while high concentrations of autotrophs in core GeoB2019-2 (Esper and Zonneveld, 2002) probably relate with low nitrate concentrations in the area of the latter core.

5.3. The Modern Analogue Technique applied on the last 25 cal ka of ODP 1233 (41°S)

The fossil dinoflagellate cyst record from core site ODP 1233 (Verleye and Louwye, 2010) was used to test the practicability of the MAT to quantify palaeoenvironmental changes in the SE Pacific (41°S) during the last 25 ka. In both the fossil and modern dataset, *Dubridinium caperatum* was grouped together with *Brigantedinium* spp.

Between 25 and 22 cal ka BP, the LGM period is characterised by intense and abrupt fluctuating MAT-based SSTs (Δ5.5 °C/200 yr), not comparable with the alkenone record of Lamy et al. (2007) (Δ3 °C/2 ka) (Fig. 12). The reason for this is the very abundant occurrence of the cosmopolitan genus *Brigantedinium* spp. during the LGM (65–85%). Today, this genus occurs in high abundances in both the Southern Ocean (e.g. Esper and Zonneveld, 2002; Harland et al., 1998), offshore Chile between 33°S and 43°S and even in the Patagonian fjords. This resulted in the selection of analogues from diverse locations covering an aSST range from 5 to 15 °C. Dependent on which region provides the most analogue samples, the estimated SSTs are substantial lower or higher, which results in highly deviating values. As *Brigantedinium* spp. includes but heterotrophic species and is capable to proliferate within a wide SST range, its abundances will most likely be influenced by the availability of its main food resources rather than by a change in SST. This makes it hazardous to make accurate quantitative SST reconstructions based on assemblages dominated by a species whose occurrences are mainly determined by some external factor not included in the calculation.

The two-step warming phase (Δ8 °C) between 18.6 and 10.7 cal ka BP corresponds with only a 2 °C increase according to the MAT. The number of analogues within a 2.5° range around ODP site 1233 increases between 18.6 and 16 cal ka BP; they do not however have an effect on the MAT-based SST values. This demonstrates that different assemblages may occur in environments with similar SST as also shown in Fig. 11 and supports the findings of Dale (1983, 1996) who observed different assemblages in coastal sites and sites from the adjacent deep-sea, without a change in SST.

The Antarctic Cold Reversal (14.4–13.2 cal ka BP) is characterised by high abundances of *Operculodinium centrocarpum* (up to 86%). According to Verleye and Louwye (2010), this period corresponds with unstable conditions caused by extreme seasonality, because of the vicinity of the

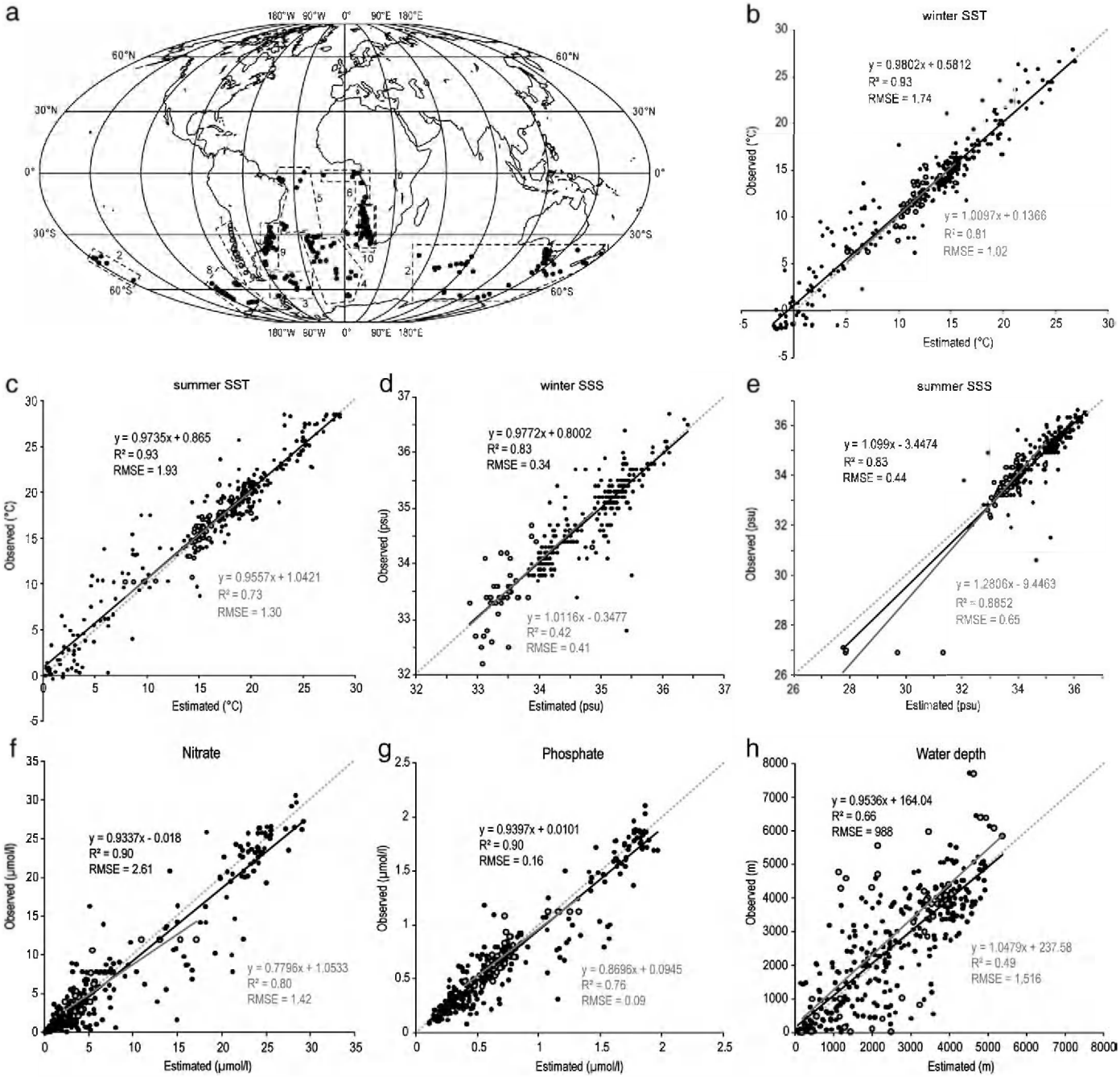

Fig. 8. (a) Locations of the 350 surface sample sites in the Southern Hemisphere, (1) SE Pacific (this study); (2) Southern Indian and Pacific Ocean (Marret and de Vernal, 1997; Marret et al., 2001); (3) Southern Ocean, Antarctica (Harland et al., 1998); (4) southern Atlantic Ocean (Esper and Zonneveld, 2002); (5) western (Sub)Equatorial Atlantic Ocean (Vink et al., 2000); (6) Gulf of Guinea (Marret, 1994); (7) Benguela upwelling area (Zonneveld et al., 2001); (8) Southern Ocean, Antarctica (Esper and Zonneveld, 2007); (9) western South Atlantic Ocean (Laurijssen and Zonneveld, unpublished); (10) Benguela upwelling area (Holzwarth et al., 2007). (b–h) Validation exercises: Estimated values plotted against observed values using the non-transformed relative abundance dataset for (b) winter SST; (c) summer SST; (d) winter SSS; (e) summer SSS; (f) nitrate; (g) phosphate; (h) water depth. Grey dots represent the SE Pacific samples, black dots represent other Southern Hemisphere samples. The regression line is given for both the SH350 database (black) and the SE Pacific database (grey), inclusive its linear equation and R^2. The RMSE for both datasets is calculated with respect to the 'y = x' regression line through the origin, visualised as a pale grey dashed line.

Subtopical Front. This time interval is interpreted differently by the MAT as a sudden increase in SST of ~5 °C. *Operculodinium centrocarpum* is a cosmopolitan species and often dominates water masses characterised by extreme seasonality (e.g. Dale, 1983) and high abundances are observed within a substantial range of SST. In the NH regions, the species often account for more than 50% of the assemblage within a SST gradient of 26 °C (Marret and Zonneveld, 2003). Species as *Operculodinium centrocarpum* make it difficult to reconstruct SST precisely and should therefore be excluded from the database. The restricted effect of SST on the geographical distribution of *Operculodinium centrocarpum* is also reflected by its contrasting concentrations in the NH high latitudes (>80%) (Marret and Zonneveld, 2003) and the SH high latitudes (<1%) (Esper and Zonneveld, 2002, 2007; Marret and de Vernal, 1997). The much higher macronutrient concentration in the latter region (Garcia et al., 2006b) is probably the main cause for the absence of the taxon around Antarctica. Including only dinoflagellate cysts with a narrow SST range or an obvious preference for warmer or colder environments such as *Bitectatodinium spongium*, *Bitectatodinium tepikiense*, *Impagidinium pallidum*, *Islandinium minutum*, *Lingulodinium machaerophorum*, *Polysphaeridium zoharyi*, *Selenopemphix antarctica* and *Spiniferites elongatus* does neither present a

Table 6
Linear equations, correlations and RMSEs of the observed versus estimated SSS and SST (winter-summer) using the MAT with the SH350 database as training set. Results for the SE Pacific surface samples and for all the SH350 sites, respectively.

Database	Data transformation	wSST			sSST			wSSS			sSSS		
		linear equation	R^2	RMSE	linear equation	R^2	RMSE	linear equation	R^2	RMSE	linear equation	R^2	RMSE
SE Pacific Database (48 samples)	% Abund	1.0097x + 0.1366	0.81	1.02	0.9557x + 1.0421	0.73	1.30	1.0116x - 0.3477	0.42	0.41	1.2806x - 9.4463	0.89	0.65
	log(% + 1)	1.0246x - 0.0168	0.79	1.07	0.9496x + 1.1514	0.71	1.35	1.12x - 3.9692	0.41	0.42	1.3259x - 10.994	0.84	1.01
	log((%x10) + 1)	0.8522x + 1.7613	0.59	1.48	0.7732x + 3.6044	0.54	1.71	0.5601x + 14.726	0.12	0.52	1.4531x - 15.376	0.71	1.31
SH Dinocyst database (350 samples)	% Abund	0.9892x + 0.5812	0.93	1.74	0.9735x + 0.865	0.93	1.93	0.9772x + 0.8002	0.83	0.34	1.099x - 3.4474	0.83	0.44
	log(% + 1)	0.994x + 0.8191	0.92	1.90	0.9555x + 1.2312	0.92	2.19	0.9835x + 0.5866	0.83	0.34	1.1123x - 3.903	0.81	0.59
	log((%x10) + 1)	0.9557x + 0.951	0.87	2.38	0.9402x + 1.4817	0.87	2.73	0.9873x + 0.4468	0.80	0.36	1.1645x - 5.7391	0.76	0.67

watertight solution for acceptable quantitative reconstructions. The relative abundances of these taxa are in turn biased by the presence of other species not depending on SST, again making it difficult to associate the relative abundances of certain species with a specific SST value.

Gradual changes in the species composition resulted in a slight shift of analogues between the early and late Holocene. However, at average 95% of the analogues were selected within a 2.5° range around ODP site 1233 during the Holocene (Fig. 12). This obviously resulted in very limited MAT-based SST variations (13–14 °C), which in this case correspond quite well with the alkenone records of Lamy et al. (2002) and Kaiser et al. (2005) (14–16 °C). However, the shifts in the assemblage composition during the Holocene were interpreted as the result of variable nutrient supply by the ACC, river input and seasonal upwelling, rather than SST changes (Verleye and Louwye, 2010). The relatively good fit between the present day MAT value and the measured SST results only from the immediate vicinity of the analogues with respect to ODP site 1233. The selection of analogues nearby ODP site 1233 may give the impression that any environmental factor can be reconstructed, even if ecological unimportant. The alkenone-based SST optima between 11.6 and 9.8 cal ka BP and around 5 cal ka BP are totally absent in the MAT reconstruction, since no other analogues were selected during these periods because restricted SST changes did not influence the cyst composition at ODP site 1233 during the Holocene. This makes it hazardous to quantify SST variations based on dinoflagellate cyst assemblages without considering the influence of other environmental parameters which might be more important on a regional scale.

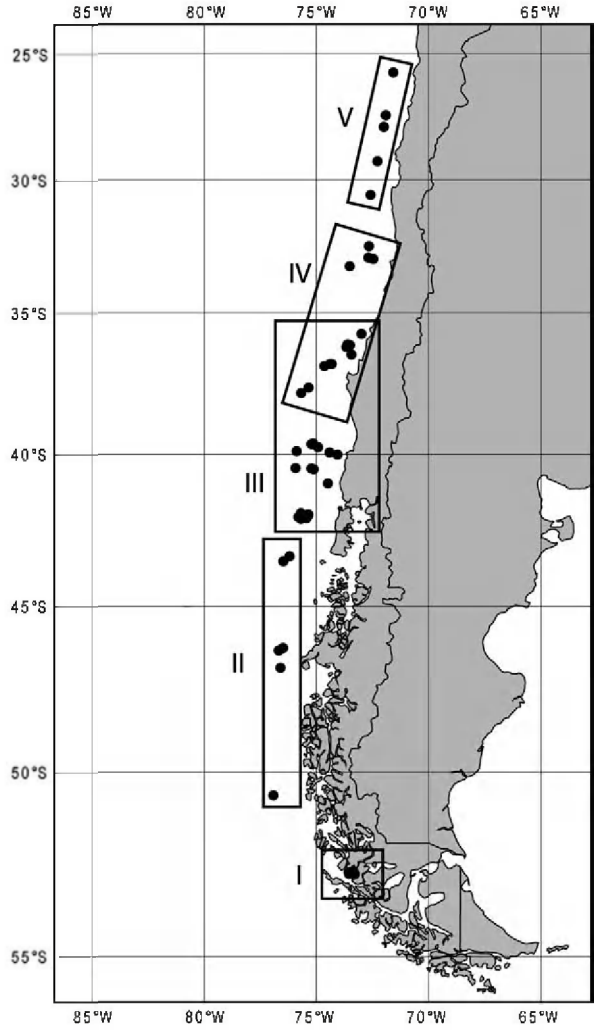

Fig. 9. The division of the SE Pacific sites in five clusters, enclosing a restricted geographical area.

6. Conclusions

The dinoflagellate cyst analysis of surface sediments offshore Chile (25–53°S) resulted in the identification of 55 taxa. In the studied area, lateral transport of cysts appears negligible, but selective degradation resulting from bacterial, chemical or mechanical decomposition could not be entirely ruled out at each site. The observed spatial distribution patterns of taxa show an obvious dominance of autotrophs in oceanic assemblages, while heterotrophic species dominate coastal assemblages. The CCA ordination diagram and the analysis of two coast–ocean transects support these observations. The cyst concentration decreases with increasing distance from the shore. Samples with the highest cyst concentrations are dominated by heterotrophic taxa and are located in the active upwelling system offshore Concepción (35–37°S). Assemblages in the upwelling areas are dominated by *Brigantedinium* spp., *Echinidinium aculeatum*, *Echinidinium granulatum/delicatum* and cysts of

Table 7
Number of analogues selected within the same geographical cluster or within a range of 2.5° longitude/latitude in the SE Pacific.

Cluster	Data transformation	Analog. within cluster (%)	Analog. within 2.5° range (%)
CLUSTER 1 (5 samples)	% Abund	68.0	68.0
	log(% + 1)	60.0	60.0
	log((%x10) + 1)	48.0	48.0
CLUSTER 2 (6 samples)	% Abund	60.0	53.3
	log(% + 1)	60.0	53.3
	log((%x10) + 1)	36.7	36.7
CLUSTER 3 (28 samples)	% Abund	92.1	80.0
	log(% + 1)	92.1	79.3
	log((%x10) + 1)	85.0	75.0
CLUSTER 4 (15 samples)	% Abund	81.3	60.0
	log(% + 1)	82.7	58.7
	log((%x10) + 1)	73.3	57.3
CLUSTER 5 (5 samples)	% Abund	32.0	24.0
	log(% + 1)	32.0	24.0
	log((%x10) + 1)	24.0	16.0
ALL CLUSTERS (48 samples)	% Abund	74.6	62.9
	log(% + 1)	74.2	61.7
	log((%x10) + 1)	63.3	55.0

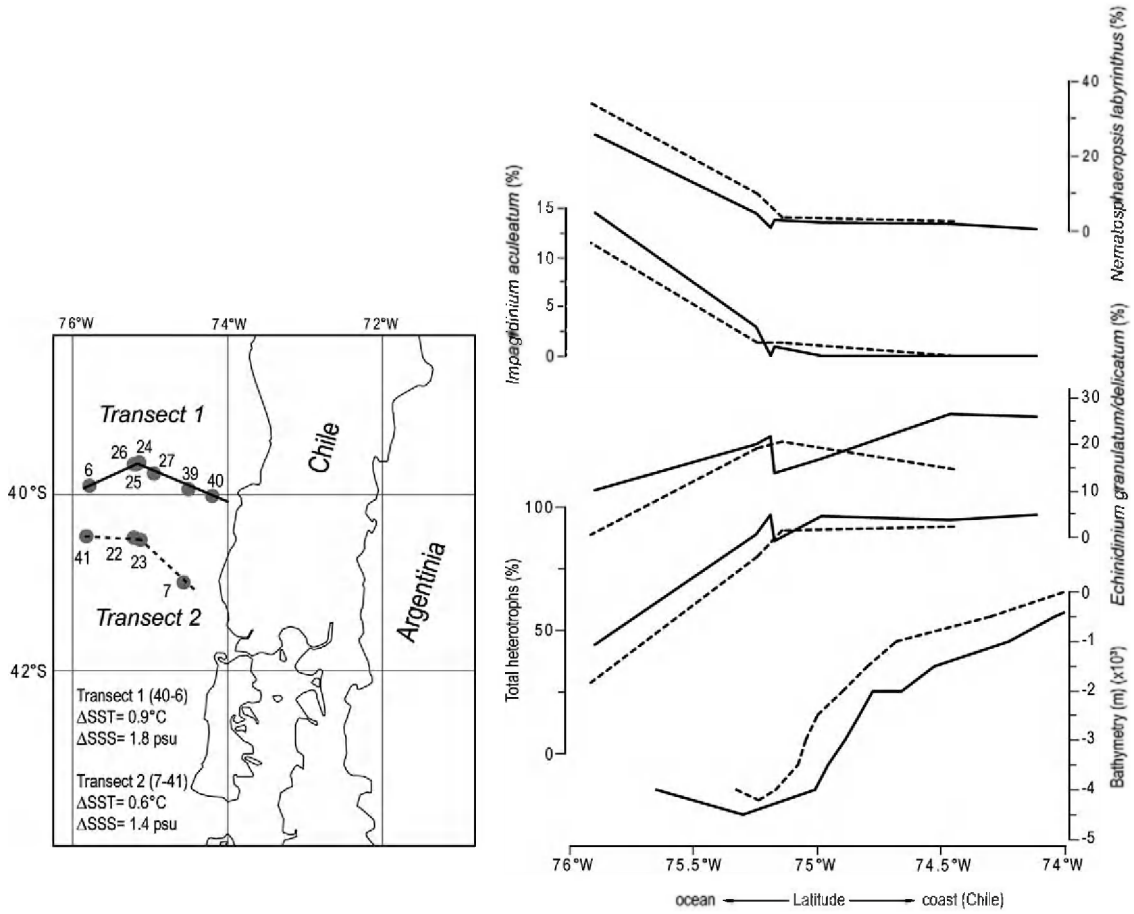

Fig. 10. (left) Positions of the two longitudinal transects with the differences in SSS and SST between the two farthest samples. (right) Changing bathymetry over both transects, the relative amount of heterotrophs, the relative abundances of the heterotrophic *Echinidinium granulatum/delicatum* and the relative abundances of the autotrophic *Impagidinium aculeatum* and *Nematosphaeropsis labyrinthus*. Transect 1 is visualised as a black line, transect 2 as a black dashed line.

Protoperidinium americanum. The best markers for the detection of active upwelling regions are *Echinidinium aculeatum* and Cyst type 11. The other protoperidinioids may also occur in high numbers in coastal areas outside upwelling cells on condition that sufficient nutrients are available; this supports the results of Dale et al. (2002). Our results highlight the importance of nutrient availability, rather than SSS and SST, as the main environmental factor controlling the relative abundances of heterotrophic taxa on a regional scale (SE Pacific).

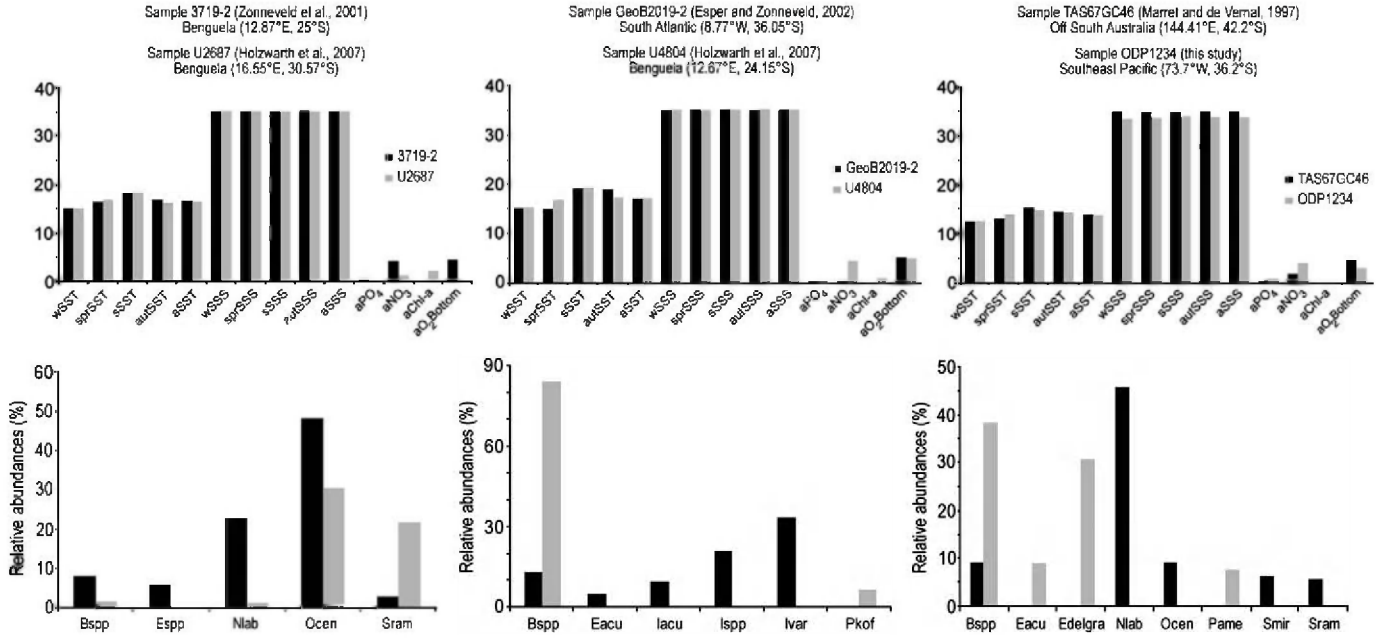

Fig. 11. Comparisons between cyst assemblages of sites characterised by similar SSS and SST, located randomly in the Southern Hemisphere.

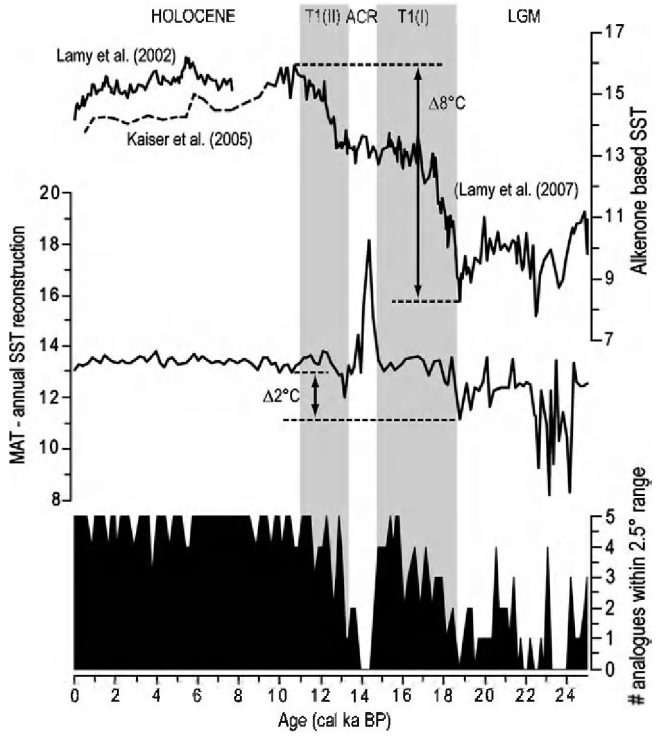

Fig. 12. Comparison between the alkenone-based SST reconstructions (Kaiser et al., 2005; Lamy et al., 2002, 2007) and the quantitative SST reconstruction based on dinoflagellate cysts using the MAT. The graph at the bottom represents the number of analogues found within a 2.5° longitude/latitude range. Abbreviations: ACR, Antarctic Cold Reversal; LGM, Last Glacial Maximum; T1(I) and T1(II), Termination 1 phase 1 and Termination 1 phase 2, respectively.

The validation exercise of the MAT results in a clustering of the analogues in the immediate vicinity of the sites for which hydrographical parameters are estimated, an observation which supports the findings of Telford (2006). Because the majority of the environmental variables remain fairly unchanged within a restricted area, almost any variable seems to be possible to reconstruct, regardless of its ecological relevance. Therefore, the validation exercise gives no information about the accuracy of the MAT results. SSS and SST undoubtedly play a prominent role in determining the spatial distribution of many dinoflagellate cyst taxa worldwide. On a regional scale, other hydrographical variables such as nutrient availability, water depth, light regime and water stability, are equally or more important. The extent to which a particular environmental variable plays a role in the spatial distribution of particular taxa is often difficult to determine. Therefore, the use of the MAT may result in strongly deviating successive quantitative reconstructions, since MAT does not consider interaction of different environmental variables.

Supplementary materials related to this article can be found online at doi:10.1016/j.palaeo.2010.10.006.

Acknowledgements

The authors thank V. Pospelova for help with the statistical treatment of the data. F. Marret is acknowledged for providing the scripts to run the MAT with the R software 2.7.0. The fruitful discussions with V. Pospelova are appreciated. We kindly acknowledge M. A. Godoi Millan who provided five surface samples from near the Strait of Magellan. Other samples were provided by the International Ocean Drilling Program (IODP) and Oregon State University (OSU). A. Gautier is acknowledged for the grammatical and stylistic corrections. Thanks also to the two anonymous reviewers, whose suggestions considerably improved the manuscript. Financial support to the first author was provided by the Institute for the Encouragement of Innovation through Science and Technology in Flanders (IWT).

Appendix A. Taxonomy and systematic palaeontology

Fifty-five species of organic-walled dinoflagellate cysts were identified in 48 core-top samples offshore Chile. Appendix A presents a list of the species recorded and a description of the morphotypes under open nomenclature.

Division DINOFLAGELLATA (Bütschli, 1885) Fensome et al., 1993
Subdivision DINOKARYOTA Fensome et al., 1993
Class DINOPHYCEAE Pascher, 1914
Subclass GYMNODINIPHYCIDAE Fensome et al., 1993
Order GYMNODINIALES Apstein, 1909
Suborder GYMNODINIINEAE (autonym)
Family GYMNODINIACEAE (Bergh 1881) Lankester 1885
Genus *Gymnodinium* Stein, 1878
Gymnodinium nolleri Ellegaard and Moestrup, 1999

Family POLYKRIKACEAE Kofoid and Swezy, 1921
Genus *Polykrikos* Bütschli, 1873
Polykrikos kofoidii Chatton, 1914
Polykrikos schwartzii Bütschli, 1873

Subclass PERIDINIPHYCIDAE Fensome et al., 1993
Order PERIDINIALES Haeckel, 1894
Suborder PERIDINIINEAE (autonym)
Family PROTOPERIDINIACEAE Balech, 1988
Subfamily PROTOPERIDINIOIDEAE Balech, 1988
Genus *Brigantedinium* Reid, 1977
Brigantedinium cariacoense Wall, 1967 ex Lentin and Williams, 1993 (grouped with *Brigantedinium* spp.)
Brigantedinium simplex Wall, 1965 ex Lentin and Williams, 1993 (grouped with *Brigantedinium* spp.)

Genus *Lejeunecysta* Artzner and Dörhöfer, 1978
Lejeunecysta spp.

Genus *Protoperidinium* (Bergh) Balech, 1974
Cyst form C Wall et al., 1977 (grouped with *Brigantedinium* spp.)
Cyst of *Protoperidinium americanum* (Gran and Braarud, 1935) Balech, 1974

Genus *Quinquecuspis* Harland, 1977
Quinquecuspis concreta (Reid, 1977) Harland, 1977

Genus *Selenopemphix* Benedek, 1972
Selenopemphix antarctica Marret and de Vernal, 1997
Selenopemphix nephroides (Benedek, 1972) Benedek and Sarjeant, 1981
Selenopemphix quanta s.l. (Bradford, 1975) Matsuoka, 1985
Selenopemphix sp. 1 (Plate 1, Fig. 10)
Description. The brown cyst has a reniform to subcircular shape in polar view. The epicyst is conical and the hypocyst has two rounded horns. The cingulum, formed by two parallel ridges with undulating margins, is deeply indented and wide (8–11 μm). The cyst wall is thin (~0.3 μm) except at the apical boss and at the tips of the antapical horns, where it thickens up to 0.9 μm. The cyst wall is shagreenate and often linear striated. The archeopyle is simple (2a) and is offset to the left of the dorsal midline. The maximum body diameter ranges between 51 (64) 77.6 μm.

Genus *Trinovantedinium* Reid, 1977
Trinovantedinium applanatum (Bradford, 1977) Bujak and Davies, 1983

Trinovantedinium variabile (Bujak, 1984) de Verteuil and Norris, 1992

Genus *Votadinium* Reid, 1977
Votadinium calvum Reid, 1977
Votadinium spinosum Reid, 1977

Subfamily PROTOPERIDINIOIDEAE Balech, 1988 or **DIPLOPSALIOIDEAE** Balech, 1988
Genus *Echinidinium* Zonneveld, 1997 ex Head et al., 2001
Echinidinium aculeatum Zonneveld, 1997
Echinidinium delicatum Zonneveld, 1997 (grouped with *Echinidinium granulatum/delicatum*)
Echinidinium granulatum Zonneveld, 1997 (grouped with *Echinidinium granulatum/delicatum*)
Echinidinium karaense Head, 2001
?Echinidinium transparantum Zonneveld, 1997
?Echinidinium zonneveldiae Zonneveld, 1997
Echinidinium sp. 3
Description. This species occurs only in very low abundances at 3 sites. The spherical cyst with a diameter of ~25 μm has a pale brown colour and bears short, solid spines between 2 and 3 μm long. The single layered wall is very thin.
Echinidinium sp. 4 (Plate 1, Fig. 6)
Description. This species is very abundant in the SE Pacific. Its relative abundances vary between 0 and 14%. The pale brown cyst is spherical with a diameter generally ranging from 25 to 33 μm, and is ornamented with long hollow spines with a length between 6 and 9 μm. The wall is thin and single layered.
Echinidinium sp. 6 (Verleye and Louwye, 2010, Supplementary Data Fig. s1, Plate Fig. 9)
Description. Echinidinium sp. 6 was observed in low abundances (<2%) in approximately one third of the samples. This pale brown spherical cyst has a diameter ranging from 30 to 35 μm. The slender spines are apiculocavate with acuminate tips, varying between 6 and 9 μm in length.

Subfamily DIPLOPSALIOIDEAE Abé, 1981
Genus *Dubridinium* Reid, 1977
Dubridinium caperatum Reid, 1977

Family PERIDINIACEAE Ehrenberg, 1831
Subfamily uncertain
Genus *Pentapharsodinium* Indelicato and Loeblich III, 1986
Pentapharsodinium dalei Indelicato and Loeblich III, 1986

Order GONYAULACALES Taylor, 1980
Suborder GONYAULACINEAE (autonym)
Family GONYAULACACEAE Lindemann, 1928
Subfamily CRIBROPERIDINIOIDEAE
Genus *Operculodinium* Wall, 1967
Operculodinium centrocarpum sensu Wall and Dale, 1966
Operculodinium israelianum (Rossignol, 1962) Wall, 1967 (short processes)

Subfamily GONYAULACOIDEAE (autonym)
Genus *Achomosphaera* Evitt, 1963
Achomosphaera spp.

Genus *Bitectatodinium* Wilson, 1973
?Bitectatodinium spongium (Zonneveld, 1997) Zonneveld and Jurkschat, 1999
Bitectatodinium tepikiense Wilson, 1973

Genus *Dalella* McMinn and Sun, 1994
Dalella chathamensis McMinn and Sun, 1994

Genus *Impagidinium* Stover and Evitt, 1978
Impagidinium aculeatum Zonneveld, 1997
Impagidinium cantabrigiense De Schepper and Head, 2008
Impagidinium japonicum Matsuoka, 1983
Impagidinium pallidum Bujak, 1984
Impagidinium paradoxum (Wall, 1967) Stover and Evitt, 1978
Impagidinium patulum (Wall, 1967) Stover and Evitt, 1978
Impagidinium plicatum Versteegh and Zevenboom, 1981
Impagidinium sphaericum (Wall, 1967) Lentin and Williams, 1981
Impagidinium strialatum (Wall, 1967) Stover and Evitt, 1978
Impagidinium sp. 1 (Plate 1, Figs. 7–9)
Description. This species was only recorded sporadically in the SE Pacific. The cyst (40–48 μm) has an ovoidal central body with an apical protuberance and a finely microgranular surface (Plate 1, Figs. 7–9). The sutural crests express tabulation but are absent in the sulcal area (Plate 1, Fig. 8). The height of the crests is more or less constant. This species is most similar to *Impagidinium paradoxum* (cyst diameter: 28–31 μm), but can easy be distinguished by its larger size.

Genus *Nematosphaeropsis* Deflandre and Cookson, 1955
Nematosphaeropsis labyrinthus (Ostenfeld, 1903) Reid, 1974

Genus *Spiniferites* Mantell, 1850
Spiniferites mirabilis (Rossignol, 1967) Sarjeant, 1970
Spiniferites ramosus (Ehrenberg, 1838) Mantell, 1854
Spiniferites sp. 1 (Verleye and Louwye, 2010, Supplementary Data Fig. s1, Plate Figs. 16–17)
Remarks. Only two poorly preserved specimens were recorded in the top sample of ODP Site 1233. Cyst body is ovoid to round. The cyst is characterised by a large membrane between the processes, but the position of the membrane could not be determined due to the poorly preserved specimens.
Spiniferites sp. 2
Remarks. Because of the poor preservation of the cyst, no description is possible. Possibly, it might be the same species as *Spiniferites* sp. 1, but the preservational state is too poor to confirm this.
Spiniferites sp. 4 (Verleye and Louwye, 2010, Supplementary Data Fig. s1, Plate Fig. 20)
Description. Spiniferites sp. 4 has a central body diameter of ~32 μm. The most prominent character of this species is the typical morphology of the processes. The processes have very broad bases, narrow upwards and trifurcate distally into long process ends, which on their turn have small recurved bifurcate tips.
Spiniferites sp. 5 (Plate Fig. 11)
Description. Spiniferites sp. 5 is a spherical cyst and has a microgranular surface. Sutural crests express tabulation, however, they are often not well preserved. Processes are always broken.

Subfamily uncertain
Genus *Pyxidinopsis* Habib, 1976
Pyxidinopsis reticulata (McMinn and Sun, 1994) Marret and de Vernal, 1997

Other undescribed dinoflagellate cysts
cf. *Achomosphaera/Spiniferites* (gonyaulacoid) (Verleye and Louwye, 2010, Supplementary Data Fig. s1, Plate Fig. 4)
Dinocyst sp. A (protoperidinioid) (Plate 1, Figs. 2–3)
Dinocyst sp. D (unknown) (Plate 1, Figs. 4–5)

References

Abrantes, F., Lopes, C., Mix, A., Pisias, N., 2007. Diatoms in Southeast Pacific surface sediments reflect environmental properties. Quaternary Science Reviews 26, 155–169.
Alves-de-Souza, C., Varela, D., Navarrete, F., Fernández, P., Leal, P., 2008. Distribution, abundance and diversity of modern dinoflagellate cyst assemblages from southern Chile (43-54°S). Botanica Marina 51, 399–410.

Anderson, N.J., 2000. Diatoms, temperature and climatic change. European Journal of Phycology 35, 307–314.

Belkin, I.M., Gordon, A.L., 1996. Southern Ocean fronts from the Greenwich meridian to Tasmania. Journal of Geophysical Research 101 (C2), 3675–3696.

Benderra, F., 1996. Palynologie et reconstitutions des conditions de surface au cours du dernier cycle climatique (140 000 ans) au site 594 du DSDP, Pacifique du sud-ouest. Master thesis, UQAM-Canada.

Biebow, N., 2003. Assemblage of dinoflagellate cysts analysed in sediment core SO78-159-1. doi:10.1594/PANGAEA.126415.

Birks, H.J.B., 1995. Quantitative palaeoenvironmental reconstructions. In: Maddy, D., Brew, J.S. (Eds.), Statistical Modelling of Quaternary Science Data. : Technical Guide 5. QRA, Cambridge, pp. 116–254.

Blumberg, S., Lamy, F., Arz, H.W., Echtler, H.P., Wiedicke, M., Haug, G.H., Oncken, O., 2008. Turbiditic trench deposits at the South-Chilean active margin: a Pleistocene-Holocene record of climate and tectonics. Earth and Planet Science Letters 268, 526–539.

Boessenkool, K.P., Brinkhuis, H., Schönfeld, J., Targarona, J., 2001a. North Atlantic sea-surface temperature changes and the climate of western Iberia during the last deglaciation; a marine palynological approach. Global and Planetary Change 30, 33–39.

Boessenkool, K.P., Van Gelder, M.-J., Brinkhuis, H., Troelstra, S., 2001b. Distribution of organic-walled dinoflagellate cysts in surface sediments from transects across the Polar Front offshore southeast Greenland. Journal of Quaternary Science 16, 661–666.

Boltovskoy, E., 1976. Distribution of recent foraminifera of the South American region. In: Hedley, R.H., Adams, C.G. (Eds.), Foraminifera. Academic Press, London, pp. 171–237.

Bouimetarhan, I., Marret, F., Dupont, L., Zonneveld, K., 2009. Dinoflagellate cyst distribution in marine surface sediments off West Africa (17-6°N) in relation to sea-surface conditions, freshwater input and seasonal coastal upwelling. Marine Micropaleontology 71, 113–130.

Boyer, T.P., Stephens, C., Antonov, J.I., Conkright, M.E., Locarnini, R.A., O'Brien, T.D., Garcia, H., 2002. World Ocean Atlas 2001. Salinity. : In: Levitus, S. (Ed.), NOAA Atlas NESDIS 50, Volume 2. U.S. Government Printing Office, Washington, D.C, p. 165. CD-ROM.

Broecker, W.S., 2003. Does the trigger for abrupt climate change reside in the ocean or in the atmosphere? Science 300, 1519–1522.

Broecker, W., Denton, G.H., 1989. The role of ocean–atmosphere reorganizations in glacial cycles. Geochimica et Cosmochimica Acta 53, 2465–2501.

Clark, P.U., Marshall, S.J., Clarke, G.K.C., Hostetler, S.W., Licciardi, J.M., Teller, J.T., 2001. Freshwater forcing of abrupt climate change during the Last Glaciation. Science 293, 283–287.

Dale, B., 1976. Cyst formation, sedimentation, and preservation: factors affecting dinoflagellate assemblages in recent sediments from Trondheimsfjord, Norway. Review of Palaeobotany and Palynology 22, 39–60.

Dale, B., 1983. In: Fryxell, A.G. (Ed.), Dinoflagellate resting cysts: 'benthic plankton'. : Survival, strategies of the algae. Cambridge University Press, New York, pp. 69–136.

Dale, B., 1996. In: Jansonius, J., McGregor, D.C. (Eds.), Dinoflagellate cyst ecology: modeling and geological applications. : Palynology: Principles and Applications, vol. 3. AASP Foundation, Dallas, TX, pp. 1249–1275.

Dale, B., 2001. The sedimentary record of dinoflagellate cysts: looking back into the future of phytoplankton blooms. Scientia Marina 65, 257–272.

Dale, A.L., Dale, B., 1992. Dinoflagellate contributions to the sediment flux of the Nordic Seas. In: Honjo, S. (Ed.), Ocean Biocoenosis Series 5. Woods Hole Oceanographic Institution Press, Woods Hole, pp. 45–76.

Dale, A.L., Dale, B., 2002. (Appendix) Application of ecologically based statistical treatments to micropalaeontology. In: Haslett, S.K. (Ed.), Quaternary Environmental Micropalaeontology. Oxford University Press Inc., New York, pp. 259–286.

Dale, B., Dale, L., Jansen, J.H.F., 2002. Dinoflagellate cysts as environmental indicators in surface sediments from the Congo deep-sea fan and adjacent regions. Palaeogeography Palaeoclimatology Palaeoecology 185, 309–338.

De Schepper, S., Head, M.J., 2008. New dinoflagellate cyst and acritarch taxa from the Pliocene and Pleistocene of the eastern North Atlantic (DSDP Site 610). Journal of Systematic Palaeontology 6, 101–117.

de Vernal, A., Hillaire-Marcel, C., 2000. Sea-ice cover, sea-surface salinity and halo-/thermocline structure of the northwest North Atlantic: modern versus full glacial conditions. Quaternary Science Reviews 19, 65–85.

de Vernal, A., Pedersen, T.F., 1997. Micropaleontology and palynology of core PAR87A–10. A 23, 000 year record of paleoenvironmental changes in the Gulf of Alaska, northeast North Pacific. Paleoceanography 12, 821–830.

de Vernal, A., Rochon, A., Hillaire-Marcel, C., Turon, J.L., Guiot, J., 1993. In: Peltier, W.R. (Ed.), Quantitative reconstruction of sea-surface conditions, seasonal extent of sea-ice cover and meltwater discharges in high latitude marine environments from dinoflagellate cyst assemblages. : Ice in the Climate System, NATO ASI Series I. Springer-Verslag, Berlin, pp. 611–621.

de Vernal, A., Turon, J.-L., Guiot, J., 1994. Dinoflagellate cyst distribution in high-latitude environments and quantitative reconstruction of sea-surface temperature, salinity and seasonality. Canadian Journal of Earth Sciences 31, 48–62.

de Vernal, A., Rochon, A., Turon, J.-L., Matthiessen, J., 1997. Organic-walled dinoflagellate cysts: palynological tracers of sea-surface conditions in middle to high latitude marine environments. Geobios 30, 905–920.

de Vernal, A., Henry, M., Matthiessen, J., Mudie, P.J., Rochon, A., Boessenkool, K.P., Eynaud, F., Grøsfjeld, K., Guiot, J., Hamel, D., Harland, R., Head, M.J., Kunz-Pirrung, M., Levac, E., Loucheur, V., Peyron, O., Pospelova, V., Radi, T., Turon, J.-L., Voronina, E., 2001. Dinoflagellate cyst assemblages as tracers of sea-surface conditions in the northern North Atlantic, Arctic and sub-Arctic seas: the new 'n = 677' data base and its application for quantitative palaeoceanographic reconstruction. Journal of Quaternary Science 16 (7), 681–698.

de Vernal, A., Eynaud, F., Henry, M., Hillaire-Marcel, C., Londeix, L., Mangin, S., Matthiessen, J., Marret, F., Radi, T., Rochon, A., Solignac, S., Turon, J.-L., 2005. Reconstruction of sea-surface conditions at middle to high latitudes of the Northern Hemisphere during the Last Glacial Maximum (LGM) based on dinoflagellate cyst assemblages. Quaternary Science Reviews 24, 897–924.

Devillers, R., de Vernal, A., 2000. Distribution of dinoflagellate cysts in surface sediments of the northern North Atlantic in relation to nutrient content and productivity in surface waters. Marine Geology 166, 103–124.

Egge, J.K., 1998. Are diatoms poor competitors at low phosphate concentrations? Journal of Marine Systems 16 (3), 191–198.

Esper, O., Zonneveld, K.A.F., 2002. Distribution of organic-walled dinoflagellate cysts in surface sediments of the Southern Ocean (eastern Atlantic sector) between the Subtropical Front and the Weddell Gyre. Marine Micropaleontology 46, 177–208.

Esper, O., Zonneveld, K.A.F., 2007. The potential of organic-walled dinoflagellate cysts for the reconstruction of past sea-surface conditions in the Southern Ocean. Marine Micropaleontology 65, 185–212.

Fensome, R.A., Williams, G.L., 2004. The Lentin and Williams Index of Fossil Dinoflagellates 2004 Edition. AASP Contributions Series, No 42. 909 pp.

Fonseca, T.R., 1989. An overview of the poleward undercurrent and upwelling along the Chilean coast. In: Neshyba, S.J., Mooers, C.N.K., Smith, R.L., Barber, R.T. (Eds.), Poleward Flows along Eastern Ocean Boundaries. New York, Springer, pp. 203–228.

Garcia, H.E., Locarnini, R.A., Boyer, T.P., and Antonov, J.I., 2006a. World Ocean Atlas 2005, Volume 3: Dissolved Oxygen, Apparent Oxygen Utilization, and Oxygen Saturation. In: Levitus, S. (Eds.), NOAA Atlas NESDIS 63, U.S. Government Printing Office, Washington, D.C., 342 pp., CD-ROM.

Garcia, H.E., Locarnini, R.A., Boyer, T.P., and Antonov, J.I., 2006b. World Ocean Atlas 2005, Volume 4: Nutrients (phosphate, nitrate, silica). In: Levitus, S. (Eds.), NOAA Atlas NESDIS 64, U.S. Government Printing Office, Washington, D.C., 396 pp., CD-ROM.

Guiot, J., 1990. In: Guiot, J., Labeyrie, L. (Eds.), Methods and programs of statistics for palaeoclimatology and palaeoecology: Quantification des changements climatiques: methode et programmes, Monographie 1, Institut National des Sciences de l'Univers (INSU-France), Paris.

Harland, R., 1983. Distribution maps of recent dinoflagellate cysts in bottom sediments from the North Atlantic Ocean and adjacent seas. Paleontology 26, 31–387.

Harland, R., Pudsey, C.J., 1999. Dinoflagellate cysts from sediment traps deployed in the Bellingshausen, Weddell and Scotia seas, Antarctica. Marine Micropaleontology 37, 77–99.

Harland, R., Pudsey, C.J., Howe, J.A., FitzPatrick, M.E.J., 1998. Recent dinoflagellate cysts in a transect from the Falkland Trough to the Weddell Sea, Antarctica. Palaeontology 41, 1093–1131.

Hebbeln, D., Marchant, M., Freudenthal, T., Wefer, G., 2000. Surface sediment distribution along the Chilean continental slope related to upwelling and productivity. Marine Geology 164, 119–137.

Hill, M.O., 1979. DECORANA—A FORTRAN Program for Detrended Correspondence Analysis and Reciprocol Averaging. Ecology and Systematics. Cornell University, New York.

Holzwarth, U., Esper, O., Zonneveld, K., 2007. Distribution of organic-walled dinoflagellate cysts in shelf surface sediments of the Benguela upwelling system in relationship to environmental conditions. Marine Micropaleontology 64, 91–119.

Imbrie, J., Boyle, E., Clemens, S.G., Duffy, A., Howard, W.R., Kukla, G., Kutzbach, J., Martinson, D.G., McIntyre, A., Mix, A., Molfino, B., Morley, J.J., Peterson, L.C., Pisias, N., Prell, W., Raymo, M., Shackleton, N.J.K., Toggweiler, J.R., 1992. On the structure and origin of major glaciations cycles, 1. Linear response to Milankovitch forcing. Paleoceanography 7, 701–738.

Imbrie, J., Berger, A., Boyle, E., Clemens, S.G., Duffy, A., Howard, W.R., Kukla, G., Kutzbach, J., Martinson, D.G., McIntyre, A., Mix, A., Molfino, B., Morley, J.J., Peterson, L.C., Pisias, N., Prell, W., Raymo, M., Schackleton, N.J.K., Toggweiler, J.R., 1993. On the structure and origin of major glaciations cycles, 2. The 100 000 yr cycle. Paleoceanography 8, 699–735.

Ingle, J.C., Keller, G., Kolpack, R.L., 1980. Benthic foraminiferal biofacies, sediments and water masses of the southern Peru-Chile Trench area, southeastern Pacific Ocean. Micropaleontology 26, 113–150.

Jackson, S.T., Williams, J.W., 2004. Modern analogues in Quaternary paleoecology: here today, gone yesterday, gone tomorrow? Annual Review of Earth and Planet Sciences 32, 495–537.

Jacobson, D.M., Anderson, D.M., 1986. Thecate heterotrophic dinoflagellates: feeding behaviour and mechanisms. Journal of Phycology 22, 249–258.

Jongman, R.H.G., ter Braak, C.J.F., Van Tongeren, O.F.R., 1987. Data analysis in community and landscape ecology, Centre for Agricultural Publishing and Documentation (Pudoc), Wageningen. 229 pp.

Kaiser, J., Lamy, F., Hebbeln, D., 2005. A 70-kyr sea-surface temperature record off southern Chile (Ocean Drilling Program Site 1233). Paleoceanography 20. doi:10.1029/2005PA001146.

Kilham, P., 1971. A hypothesis concerning silica and the freshwater planktonic diatoms. Limnology and Oceanography 16 (1), 10–18.

Knorr, G., Lohmann, G., 2003. Southern Ocean origin for the resumption of Atlantic thermohaline circulation during deglaciation. Nature 424, 532–536.

Lamy, F., Hebbeln, D., Röhl, U., Wefer, G., 2001. Holocene rainfall variability in southern Chile: a marine record of latitudinal shifts of the Southern Westerlies. Earth and Planetary Science Letters 185, 369–382.

Lamy, F., Rühlemann, C., Hebbeln, D., Wefer, G., 2002. High- and low-latitude climate control on the position of the southern Peru–Chile Current during the Holocene. Paleoceanography 17 (2). doi:10.1029/2001PA000727.

Lamy, F., Kaiser, J., Arz, H.W., Hebbeln, D., Ninnemann, U., Timm, O., Timmermann, A., Toggweiler, J.R., 2007. Modulation of the bipolar seesaw in the Southeast Pacific during Termination 1. Earth and Planetary Science Letters 259, 400–413.
Lignum, J., Jarvis, I., Pearce, M.A., 2008. A critical assessment of standard processing methods for the preparation of palynological samples. Review of Palaeobotany and Palynology 149, 133–149.
Louwye, S., Head, M.J., De Schepper, S., 2004. Palaeoenvironment and dinoflagellate cyst stratigraphy of the Pliocene in northern Belgium at the southern margin of the North Sea Basin. Geological Magazine 141 (3), 353–378.
Marret, F., 1994. Distribution of dinoflagellate cysts in recent marine sediments from the east Equatorial Atlantic (Gulf of Guinea). Review of Palaeobotany and Palynology 84, 1–22.
Marret, F., de Vernal, A., 1997. Dinoflagellate cyst distribution in surface sediments of the southern Indian Ocean. Marine Micropaleontology 29, 367–392.
Marret, F., Zonneveld, K.A.F., 2003. Atlas of modern organic-walled dinoflagellate cyst distribution. Review of Palaeobotany and Palynology 125, 1–200.
Marret, F., de Vernal, A., Benderra, F., Harland, R., 2001. Late Quaternary sea-surface conditions at DSDP Hole 594 in the southwest Pacific Ocean based on dinoflagellate cyst assemblages. Journal of Quaternary Science 16 (7), 739–751.
Matsuoka, K., Kawami, H., Nagai, S., Iwataki, M., Takayama, H., 2009. Re-examination of cyst-motile relationship of *Polykrikos kofoidii* Chatton and *Polykrikos schwartzii* Bütschli (Gymnodiniales, Dinophyceae). Review of Palaeobotany and Palynology 154, 79–90.
Matthiessen, J., 1995. Distribution patterns of dinoflagellate cysts and other organic-walled microfossils in recent Norwegian–Greenland Sea sediments. Marine Micropaleontology 24, 307–334.
McMinn, A., 1992. Pliocene through Holocene dinoflagellate cyst biostratigraphy of the Gippsland Basin, Australia. In: Head, M., Wrenn, J. (Eds.), Neogene and Quaternary dinoflagellate cysts and acritarchs. AASP, Dallas, pp. 141–161.
McMinn, A., 1995. Why are there no post-Palaeogene dinoflagellate cysts in the Southern Ocean? Micropaleontology 41, 383–386.
McMinn, A., Sun, X., 1994. Recent dinoflagellate cysts from the Chatham Rise, Southern Ocean, East of New Zealand. Palynology 18, 41–53.
McMinn, A., Wells, P., 1997. Use of dinoflagellate cysts to determine changing Quaternary sea-surface temperature in southern Australia. Marine Micropaleontology 29, 407–422.
Mertens, K.N., Verhoeven, K., Verleye, T., Louwye, S., Amorim, A., Ribeiro, S., Deaf, A.S., Harding, I.C., De Schepper, S., González, C., Kodrans-Nsiah, M., de Vernal, A., Henry, M., Radi, T., Dybkjaer, K., Poulsen, N.E., Feist-Burkhardt, S., Chitolie, J., Heilmann-Clausen, C., Londeix, L., Turon, J.-L., Marret, F., Matthiessen, J., McCarthy, F.M.G., Prasad, V., Pospelova, V., Hughes, J.E.K., Riding, J.B., Rochon, A., Sangiorgi, F., Welters, N., Sinclair, N., Thun, C., Soliman, A., Van Nieuwenhove, N., Vink, A., Young, M., 2009. Determining the absolute abundance of dinoflagellate cysts in recent marine sediments: the *Lycopodium* marker-grain method put to the test. Review of Palaeobotany and Palynology 157, 238–252.
Mudie, P.J., 1992. Circum-Arctic Quaternary and Neogene marine palynofloras: paleoecology and statistical analysis. In: Head, M.J., Wrenn, J.H. (Eds.), Neogene and Quaternary Dinoflagellate Cysts and Acritarchs. AASP Foundation, Dallas, TX, pp. 347–390.
Murray, J.W., 2001. The niche of benthic foraminifera, critical thresholds and proxies. Marine Micropaleontology 41, 1–7.
Palma, S., Silva, N., 2004. Distribution of siphonophores, chaetognaths, euphausiids and oceanographic conditions in the fjords and channels of southern Chile. Deep-Sea Research II 51, 513–535.
Pitcher, G.C., Joyce, L.B., 2009. Dinoflagellate cyst production on the southern Namaqua shelf of the Benguela upwelling system. Journal of Plankton Research 31 (8), 865–875.
Pospelova, V., de Vernal, A., Pedersen, T.F., 2008. Distribution of dinoflagellate cysts in surface sediments from the northeastern Pacific Ocean (43-25°N) in relation to sea-surface temperature, salinity, productivity and coastal upwelling. Marine Micropaleontology 68, 21–48.
R Development Core Team, 2008. R: A language and environment for statistical computing, version 2.7.0., Vienna, Austria.
Rochon, A., de Vernal, A., Turon, J.-L., Matthiessen, J., Head, M.J., 1999. Distribution of recent dinoflagellate cysts in surface sediments from the North Atlantic Ocean and adjacent seas in relation to sea-surface parameters: AASP Contribution Series, 35, p. 146.
Salter, J., Murray, B.G., Braggins, J.E., 2002. Wettable and unsinkable: the hydrodynamics of saccate pollen grains in relation to the pollination mechanism in the two New Zealand species of *Prumnopitys* Phil. (Podocarpaceae). Annals of Botany 89, 133–144.
Seidov, D., Maslin, M., 2001. Atlantic Ocean heat privacy and the bipolar climate seesaw during Heinrich and Dansgaard-Oeschger events. Journal of Quaternary Science 16 (4), 321–328.
Shaffer, G., Hormazabal, S., Pizarro, O., Salinas, S., 1999. Seasonal and interannual variability of currents and temperature off central Chile. Journal of Geophysical Research 104 (29), 29,951–29,961.
Shaffer, G., Hormazabal, S., Pizarro, O., Ramos, M., 2004. Circulation and variability in the Chile Basin. Deep Sea Research, Part I 51 (10), 1367–1386.
Sprangers, M., Dammers, N., Brinkhuis, H., van Weering, T.C.E., Lotter, A.F., 2004. Modern organic-walled dinoflagellate cyst distribution offshore NW Iberia; tracing the upwelling system. Review of Palaeobotany and Palynology 128, 97–106.
Stephens, C., Antonov, J.I., Boyer, T.P., Conkright, M.E., Locarnini, R.A., O'Brien, T.D., and Garcia, H.E., 2002. World Ocean Atlas 2001, Volume 1: Temperature. In: Levitus, S. (Eds.), NOAA Atlas NESDIS 49, U.S. Government Printing Office, Washington, D.C., 167 pp., CD-ROM.
Stocker, R.F., Wright, D.G., 1991. Rapid transitions of the oceans deep circulation induced by changes in surface water fluxes. Nature 351, 729–732.
Stockmarr, J., 1971. Tablets with spores used in absolute pollen analysis. Pollen et Spores 13, 615–621.
Strub, P.T., Mesias, J.M., Montecino, V., Ruttlant, J., Salinas, S., 1998. Coastal ocean circulation off western South America. In: Robinson, A.R., Brink, K.H. (Eds.), The Global Coastal Ocean: Regional Studies and Syntheses. John Wiley, New York, pp. 273–315.
Susek, E., Zonneveld, K.A.F., Fischer, G., Versteegh, G.J.M., Willems, H., 2005. Organic-walled dinoflagellate cyst production in relation to upwelling intensity and lithogenic influx in the Cape Blanc region (off north-west Africa). Phycological Research 53, 97–112.
Telford, R.J., 2006. Limitations of dinoflagellate cyst transfer functions. Quaternary Science Reviews 25, 1375–1382.
Telford, R.J., Birks, H.J.B., 2005. The secret assumption of transfer functions: problems with spatial autocorrelation in evaluating model performance. Quaternary Science Reviews 24, 2173–2179.
Telford, R.J., Birks, H.J.B., 2009. Evaluation of transfer functions in spatially structured environments. Quaternary Science Reviews 28, 1309–1316.
ter Braak, C.J.F., 1986. Canonical correspondence analysis: a new eigenvector technique for multivariate direct gradient analysis. Ecology 67, 1167–1197.
ter Braak, C.J.F., 1987. The analysis of vegetation–environment relationships by canonical correspondence analysis. Vegetatio 69, 69–77.
ter Braak, C.J.F., 1995. In: Jongman, R.H.G., ter Braak, C.J.F., van Tongeren, O.F.R. (Eds.), Ordination. : Data Analysis in Community and Landscape Ecology. Cambridge University Press, pp. 91–171.
ter Braak, C.J.F., Prentice, I.C., 1988. A theory of gradient analysis. Advances in Ecological Research 18, 271–317.
ter Braak, C.J.F., Šmilauer, P., 1998. CANOCO reference manual and users guide to Canoco for Windows: software for canonical community ordination (version 4). Microcomputer Power, Ithaca, New York.
Turon, J.-L., 1984. Le palynoplancton dans l'environnement actuel de l'Atlantique nord-oriental. Evolution climatique et hydrologique depuis le dernier maximum glaciaire. Mémoire de l'Institut de Géologie du basin d'Aquitaine. Bordeaux, 17, 313 pp.
Valdenegro, A., Silva, S., 2003. Physical and chemical oceanographic features of inlets and fjords of Southern Chile, between Magellan Strait and Cape Horn (Cimar 3 Fiordos). Ciencia y Tecnologia del Mar 26 (2), 19–57.
Verleye, T.J., Louwye, S., 2010. Late Quaternary environmental changes and latitudinal shifts of the Antarctic Circumpolar Current as recorded by dinoflagellate cysts from offshore Chile (41°S). Quaternary Science Reviews 29, 1025–1039.
Vidal, L., Schneider, R.R., Marchal, O., Bickert, T., Stocker, T.F., Wefer, G., 1999. Link between the North and South Atlantic during the Heinrich events of the last glacial period. Climate Dynamics 15, 909–919.
Villa-Martínez, R., Moreno, P.I., 2007. Pollen evidence for variations in the southern margin of the westerly winds in SW Patagonia over the last 12, 600 years. Quaternary Research 68, 400–409.
Vink, A., Zonneveld, K.A.F., Willems, H., 2000. Organic-walled dinoflagellate cysts in western equatorial Atlantic surface sediments: distribution and their relation to environment. Review of Palaeobotany and Palynology 112, 247–286.
Voronina, E., Polyak, L., de Vernal, A., Peyron, O., 2001. Holocene variations of sea-surface conditions in the southeastern Barents Sea, reconstructed from dinoflagellate cyst assemblages. Journal of Quaternary Science 16, 717–726.
Wall, D., Dale, B., Lohmann, G.P., Smith, W.K., 1977. The environmental and climatic distribution of dinoflagellate cysts in modern marine sediments from regions in the North and South Atlantic oceans and adjacent seas. Marine Micropaleontology 2, 121–200.
Weaver, A.J., Saenko, O.A., Clark, P.U., Mitrovica, J.X., 2003. Meltwater pulse 1A from Antarctica as a trigger of the Bølling-Allerød warm interval. Science 299, 1709–1713.
Whittaker, R.H., 1973a. Ordination and Classification of Communities. Junk Publishers, The Hague.
Whittaker, R.H., 1973b. Niche, habitat, and ecotype. The American Naturalist 107, 321–338.
Zonneveld, K.A.F., 1997. Dinoflagellate cyst distribution in surface sediments of the Arabian Sea (Northwestern Indian Ocean) in relation to temperature and salinity gradients in the upper water column. Deep-Sea Research II 44, 1411–1443.
Zonneveld, K.A.F., Brummer, G.-J.A., 2000. (Palaeo-)ecological significance, transport and preservation of organic-walled dinoflagellate cysts in the Somali Basin, NW Arabian Sea. Deep-Sea Research II 47, 2229–2256.
Zonneveld, K.A.F., Versteegh, G.J.M., de Lange, G.J., 1997. Preservation of organic-walled dinoflagellate cysts in different oxygen regimes: a 10, 000 year natural experiment. Marine Micropaleontology 29, 393–405.
Zonneveld, K.A.F., Hoek, R.P., Brinkhuis, H., Willems, H., 2001. Geographical distributions of organic-walled dinoflagellate cysts in surficial sediments of the Benguela upwelling region and their relationship to upper ocean conditions. Progress in Oceanography 48, 25–72.